Luminant

Rafael Flores
Senior Vice President &
Chief Nuclear Officer
rafael.flores@luminant.com

Luminant Power
P O Box 1002
6322 North FM 56
Glen Rose, TX 76043

T 254.897.5590
F 254.897.6652
C 817.559.0403

CP-200901534
Log # TXNB-09059

Ref. # 10 CFR 52

October 28, 2009

U. S. Nuclear Regulatory Commission
Document Control Desk
Washington, DC 20555
ATTN: David B. Matthews, Director
Division of New Reactor Licensing

SUBJECT: COMANCHE PEAK NUCLEAR POWER PLANT, UNITS 3 AND 4
DOCKET NUMBERS 52-034 AND 52-035
FINAL RESPONSES TO REQUESTS FOR ADDITIONAL INFORMATION
NO. 1889, 2929, AND 2930

Dear Sir:

Luminant Generation Company LLC (Luminant) herein submits the final responses to Requests for Additional Information (RAI) No. 1889, 2929, and 2930 for the Combined License Application for Comanche Peak Nuclear Power Plant Units 3 and 4. The affected Final Safety Analysis Report pages are included with the responses. The specific questions answered are:

RAI	1889 (CP RAI #11)	2929 (CP RAI #22)	2930 (CP RAI #19)
	02.05.02-1	02.05.04-1	02.05.05-1
	02.05.02-3	02.05.04-2	
		02.05.04-3	
		02.05.04-4	
		02.05.04-9	
		02.05.04-10	
		02.05.04-17	

This submittal completes Luminant's responses to RAIs in FSAR Section 2.5, "Geology, Seismology, and Geotechnical Engineering." Should you have any questions regarding these responses, please contact Don Woodlan (254-897-6887, Donald.Woodlan@luminant.com) or me.

There are no commitments in this letter.

I state under penalty of perjury that the foregoing is true and correct. Executed on October 28, 2009.

Sincerely,

Luminant Generation Company LLC

Donald R Woodlan for

Rafael Flores

D090

NRO

Attachments
1. Response to Request for Additional Information No. 1889 (CP RAI #11)
2. Response to Request for Additional Information No. 2929 (CP RAI #22)
3. Response to Request for Additional Information No. 2930 (CP RAI #19)
4. TXUT-001-FSAR-2 5-CALC-009 Rev.1 - Settlement and Bearing Capacity (on CD)

cc: Stephen Monarque w/all Attachments (on CD)

Electronic Distribution w/Attachments 1-3

mike.blevins@luminant.com
Rafael.Flores@luminant.com
mlucas3@luminant.com
jeff.simmons@energyfutureholdings.com
Bill.Moore@luminant.com
Brock.Degeyter@energyfutureholdings.com
rbird1@luminant.com
Matthew.Weeks@luminant.com
Allan.Koenig@luminant.com
Timothy.Clouser@luminant.com
Ronald.Carver@luminant.com
David.Volkening@luminant.com
Bruce.Turner@luminant.com
Eric.Evans@luminant.com
Robert.Reible@luminant.com
donald.woodlan@luminant.com
John.Conly@luminant.com
JCaldwell@luminant.com
David.Beshear@txu.com
Ashley.Monts@luminant.com
Fred.Madden@luminant.com
Dennis.Buschbaum@luminant.com
Carolyn.Cosentino@luminant.com

Luminant Records Management –
Portfolio of .pdf files

masahiko_kaneda@mnes-us.com
masanori_onozuka@mnes-us.com
ck_paulson@mnes-us.com
joseph_tapia@mnes-us.com
russell_bywater@mnes-us.com
diane_yeager@mnes-us.com
kazuya_hayashi@mnes-us.com
mutsumi_ishida@mnes-us.com
nan_sirirat@mnes-us.com
rjb@nei.org
kak@nei.org
michael.takacs@nrc.gov
cp34update@certrec.com
michael.johnson@nrc.gov
David.Matthews@nrc.gov
Balwant.Singal@nrc.gov
Hossein.Hamzehee@nrc.gov
Stephen.Monarque@nrc.gov
jeff.ciocco@nrc.gov
michael.willingham@nrc.gov
john.kramer@nrc.gov
Brian.Tindell@nrc.gov
Elmo.Collins@nrc.gov
Loren.Plisco@nrc.com
Laura.Goldin@nrc.gov
James.Biggins@nrc.gov
Susan.Vrahoretis@nrc.gov
sfrantz@morganlewis.com
tmatthews@morganlewis.com

Attachment 1

Response to Request for Additional Information No. 1889 (CP RAI #11)

RESPONSE TO REQUEST FOR ADDITIONAL INFORMATION

Comanche Peak, Units 3 and 4

Luminant Generation Company LLC

Docket Nos. 52-034 and 52-035

RAI NO.: 1889 (CP RAI #11)

SRP SECTION: 02.05.02 – Vibratory Ground Motion

QUESTIONS for Geosciences and Geotechnical Engineering Branch 1 (RGS1)

DATE OF RAI ISSUE: 7/1/2009

QUESTION NO.: 02.05.02-1

In FSAR Subsection 2.5.2.1.2 you stated that the updated earthquake catalog covers an area bounded by 28° N to 38° N and 93° W to 104° W. The update area does not completely cover all of the EPRI seismic sources used in your hazard calculations. Please justify the use of a limited spatial extent in your earthquake catalog update for the Comanche Peak site. Please describe how you account for any earthquakes occurring since 1985 within the EPRI sources, but outside of the area of your update that might potentially impact seismic source parameters used in hazard calculations at the Comanche Peak site.

ANSWER:

Due to this RAI question, a supplemental earthquake catalog (referred to here as the "supplemental catalog") was compiled that encompasses all of the contributing EPRI-SOG source zones for the Comanche Peak site (see FSAR Tables 2.5.1-206 through 2.5.1-211) outside of the area included in the Comanche Peak updated seismicity catalog (referred to here as the "updated catalog") (see FSAR Section 2.5.2.1.2). The explicit purpose of compiling the supplemental was to determine whether any earthquakes occur within contributing EPRI-SOG zones, yet outside of the updated Comanche Peak catalog extent, that have magnitudes greater than the lower-bound maximum magnitude (Mmax) for the source zone containing the earthquake. Earthquakes within the updated catalog with magnitudes greater than the lower-bound Mmax of their host zone are addressed in FSAR Section 2.5.2.4.2.2 and the response to Question 02.05.02-4 of RAI No. 1889 (CP RAI #11) provided via Luminant letter TXNB-09042 dated September 10, 2009 (ML092580684).

The supplemental catalog was compiled using web-based searches of the Advanced National Seismic System (ANSS) catalog (http://www.ncedc.org/anss/catalog-search.html) and the US Geological Survey National Earthquake Information Center (NEIC) catalog. All earthquakes from these catalogs occurring between 1 January 1985 and 12 December 2006 with magnitude greater than or equal to 4.5 and located within 55º to 111º W and 24º to 55º N were extracted from the source catalogs and combined into the supplemental catalog by identifying and removing duplicate events, with the largest magnitude event retained. Note that magnitudes were not converted to a common scale, as this calculation is only intended to identify those sources that have a potential Mmax conflict with observed seismicity.

Based on the supplemental catalog, there are two zones with earthquakes outside of the updated catalog region that have magnitudes greater than the lower-bound Mmax for their host zones. These zones and the associated earthquakes are:

- Law zone 26 (Oklahoma Aulacogen-Arbuckle Wichita Rift)
  - The 10 August 2005 Mw 5.0 (Emb ~ 5.4) earthquake in northern New Mexico (Figure 1)
- Rondout zone C02 (Grenville Crust)
  - The 11 November 1988 Mw 5.9 Saguenay earthquake in Quebec (Figure 2); and
  - The 25 September 1998 mb 5.2 Pymatuning earthquake in western Pennsylvania (Figure 2).

The potential impact of the earthquakes in both zones is discussed below.

<u>Law Zone 26</u>

Law zone 26 represents the Oklahoma Aulacogen – Arbuckle Uplift. The 10 August 2005 Mw 5.0 (Emb ~ 5.4) earthquake occurred in the easternmost extent of the zone (Figure 1). This earthquake could have a potential impact on the Mmax distribution for the zone 26 because it has a magnitude larger than the lower-bound Mmax for the zone (magnitudes and weights of mb 5.0 [0.2], 5.2 [0.5], and 6.8 [0.3]) (see FSAR Table 2.5.2-204). A sensitivity analysis was conducted to determine the potential impact on the hazard at Comanche Peak from changing the Mmax distribution for the zone based on this earthquake. A modified Mmax distribution of mb 5.4 [0.7] and 6.8 [0.3] was used in the analysis that is based on the original Mmax distribution for the zone and the Law methodology for prescribing Mmax. The sensitivity analysis demonstrated that at 10 Hz and 1 Hz spectral accelerations, the modified Mmax distribution would increase the mean rock hazard at very low amplitudes, but would not change the mean rock hazard for amplitudes where the annual frequency of exceedence is 1E-3 or less. Therefore, there would be no change in design ground motions (which are based on amplitudes with annual frequencies of 1E-4 and less) resulting from modifying the Mmax distribution for zone 26 based on this earthquake.

<u>Rondout Zone C02 (Grenville Crust)</u>

Rondout zone C02 is a combination of five individual source zones representing Grenville age crust that are referred to in the Rondout EPRI-SOG volume as zone 50. The Rondout team describes the zones as follows:

> "<u>Seismic zone #50-Grenville Crust</u>. (background) The remaining areas not included in seismic source zones that are in the Grenville (1.1 b.y.) age crust. This was separated from other PreCambrian crust because there appears to be a higher level of background seismicity here" (volume 10, page B19-B20) (EPRI, 1986-1989).

This passage indicates that zone C02 is a background zone that was created as a default for all of the "leftover pieces" of CEUS crust that Rondout did not identify as a unique source zone. As such, the five different zones that make up zone C02 are not combined into a source zone by any geologic, tectonic or geophysical characteristic that Rondout used to define source characteristics. Based on the Rondout methodology and the fact that both the Saguenay and Pymatuning earthquakes are at great distances from the Comanche Peak site (2800 km and 1800 km, respectively) and in different zone C02 polygons than that hosting the site (Figure 2), it was determined that these earthquakes do not have any implications for the Mmax distributions used for Comanche Peak. This conclusion is also supported by research on the Saguenay earthquake that has shown the earthquake is most likely related to faults associated with the lapetan St. Lawrence rift (Adams and Basham, 1991; Atkinson, 2007; Hasegawa, 1991; Roy et al., 1993), and thus the zone containing this earthquake represents a distinctly different tectonic setting and geologic history than that experienced by the crust surrounding the site.

References:

Adams, J., and Basham, P., 1991, The siesmicity and seismotectonics of eastern Canada, in Slemmons, D.B., Engdahl, E., Zoback, M.D., and Blackwell, D.D., eds., Neotectonics of North America, Volume 1: Boulder, CO, Geological Society of America, p. 261-276.

Atkinson, G., 2007, Challenges in seismic hazard analysis for contential interiors, in Stein, S., and Mazzotti, S., eds., Continental Intraplate Earthquakes: Science, Hazard, and Policy Issues: Boulder, CO, Geological Scociety of America, Special Paper 425, p. 329-344.

EPRI, 1986-1989, Seismic hazard Methodology for the Central and Eastern United States (NP-4726), Vol. 1-3 & 5-10, Electric Power Research Institute (EPRI).

Hasegawa, H.S., 1991, Four seismogenic environments in eastern Canada: Tectonophysics, v. 186, p. 3-17.

Roy, D.W., Schmitt, L., Woussen, G., and DuBerger, R., 1993, Lineaments from Airborne SAR Images and the 1988 Saguenay Earthquake, Quebec, Canada: Photogrammetric Engineering & Remote Sensing, v. 59, p. 1299-1305.

Impact on R-COLA

None.

Impact on S-COLA

None.

Impact on DCD

None.

Attachments

Figure 1 - Contributing EPRI-SOG source zones for the Law team with earthquakes from the supplemental catalog

Figure 2 - Contributing EPRI-SOG source zones for the Rondout team with earthquakes from the supplemental catalog

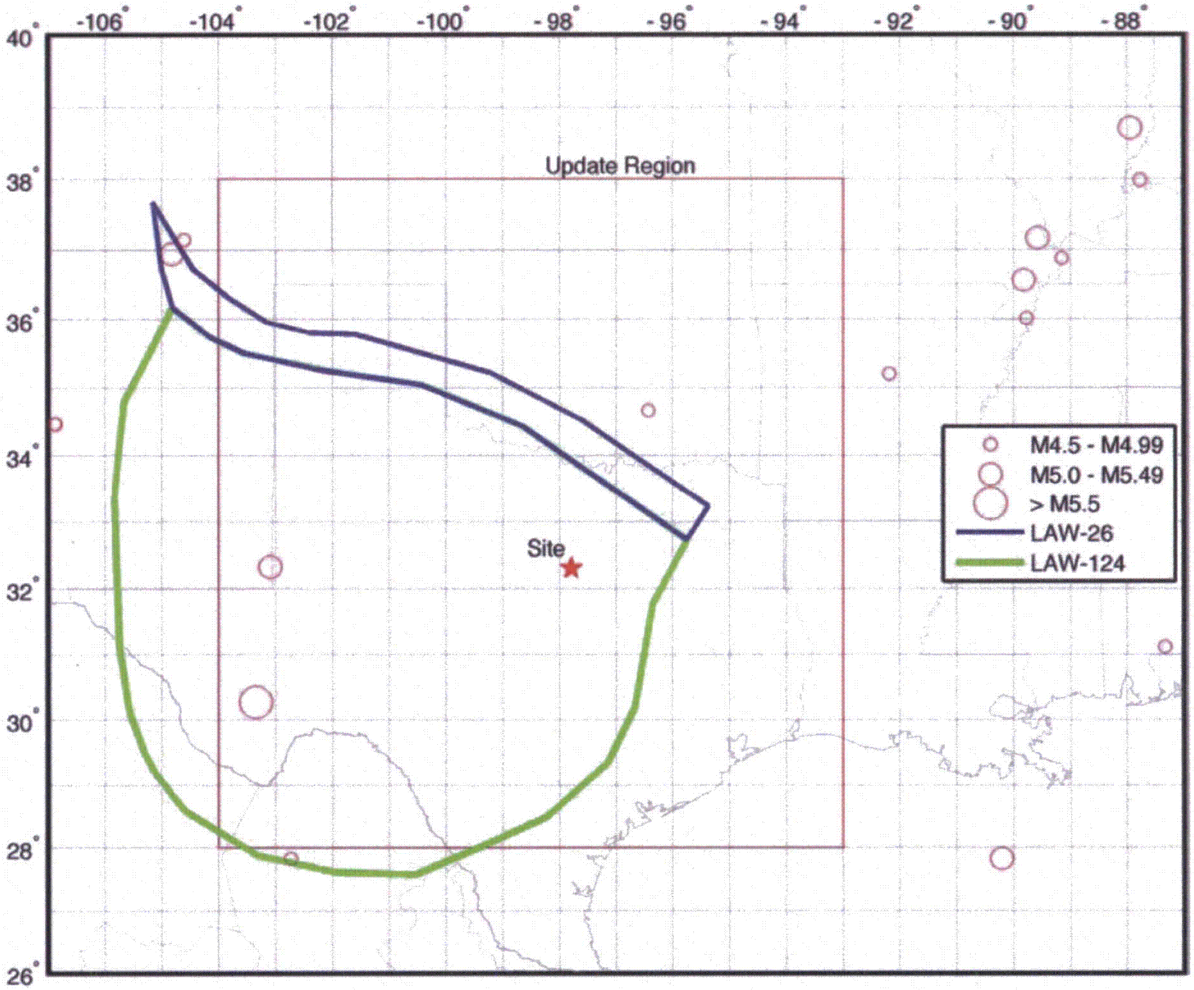

2.5.2-1 Figure 1: Contributing EPRI-SOG source zones for the Law team with earthquakes from the supplemental catalog (red circles). Region of updated catalog is shown as red box. The 10 August 2005 Mw 5.0 (Emb 5.4) earthquake in northern New Mexico is the earthquake located in the furthest northwest region of the zone 26.

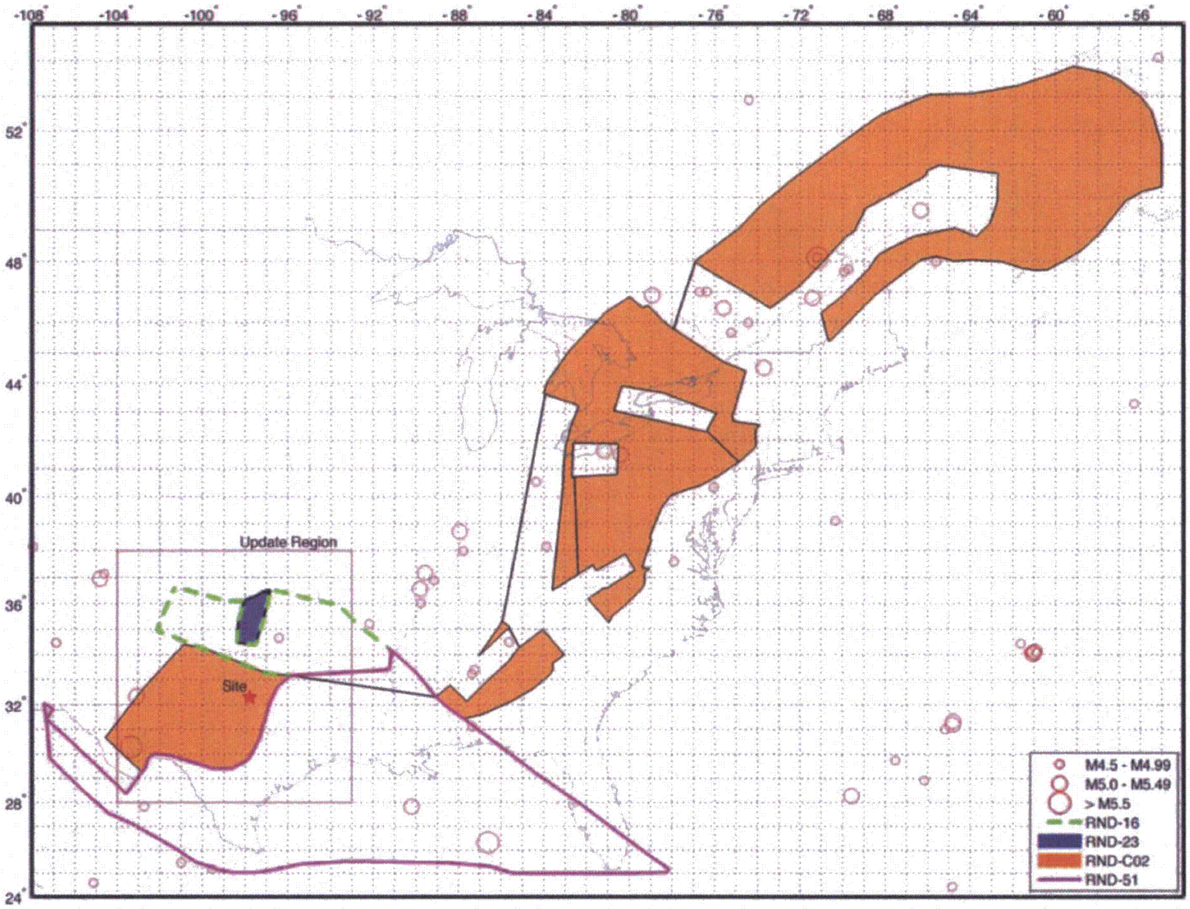

2.5.2-1 Figure 2: Contributing EPRI-SOG source zones for the Rondout team with earthquakes from the supplemental catalog (red circles). Region of updated catalog is shown as red box. The Mw 5.9 Saguenay earthquake is located in southern Quebec at -71.2° E and 48.1° N in the northernmost polygon of zone C02. The mb 5.2 Pymatuning earthquake is located in western Pennsylvania at -80.4° E and 41.5° N in the second northernmost polygon of zone C02.

RESPONSE TO REQUEST FOR ADDITIONAL INFORMATION

Comanche Peak, Units 3 and 4

Luminant Generation Company LLC

Docket Nos. 52-034 and 52-035

RAI NO.: 1889 (CP RAI #11)

SRP SECTION: 02.05.02 – Vibratory Ground Motion

QUESTIONS for Geosciences and Geotechnical Engineering Branch 1 (RGS1)

DATE OF RAI ISSUE: 7/1/2009

QUESTION NO.: 02.05.02-3

In Subsection 2.5.2.4.2.1 you described the results of a sensitivity study to determine whether the original earthquake recurrence rates used in the 1989 EPRI study still apply to the seismic sources used in the Comanche Peak PSHA study. Your sensitivity study focused on two test zones rather than the actual EPRI seismic source geometries. Please explain why the conclusions reached by using these two test zones are applicable to all of the EPRI seismic sources used for the Comanche Peak site, especially considering that seismic sources, in general, are independent of each other.

ANSWER:

FSAR Figures 2.5.2-223 through 2.5.2-228 show contributions to seismic hazard by magnitude and distance for high- and low-frequency ground motions corresponding to mean annual frequencies of exceedence of 10^{-4}, 10^{-5}, and 10^{-6}. These plots indicate that three sources of earthquakes contribute virtually all seismic hazard at the site: (a) local earthquakes within 40 km of the site, (b) earthquakes on the Meers fault, located about 270 km from the site, and (c) earthquakes in the New Madrid seismic zone, located between 800 and 1000 km from the site. Earthquakes on the Meers fault are characterized by magnitudes and mean recurrence rates based on geologic studies of fault geometry and Holocene units displaced by the fault. Earthquakes in the New Madrid seismic zone are characterized by magnitudes based on fault geometry and on the 1811-1812 sequence, and mean recurrence rates based on paleoliquefaction evidence from sand blows with datable deposits used to estimate the number and period over which multiple earthquake sequences have occurred. Thus the updated catalog is used to evaluate the characteristics of earthquake occurrences in the EPRI seismic sources, since the characteristics of earthquakes on the Meers fault and in the New Madrid seismic zone are determined from geologic studies of these potential earthquake sources.

For the EPRI seismic sources, FSAR Figures 2.5.2-223 through 2.5.2-228 indicate that earthquakes must occur within 40 km of the site to contribute significantly to seismic hazard at ground motions corresponding to mean annual frequencies of exceedence of 10^{-4}, 10^{-5}, and 10^{-6}. For this reason, Test Area 1 (shown in FSAR Figure 2.5.2-209) was drawn to concentrate on local seismicity. Because historical seismicity in the vicinity of the site is sparse, Test Area 1 was expanded to encompass seismicity within about 150 km of the site. In addition, it was recognized that more historical seismicity has occurred north of the site in central Oklahoma than has occurred in the direct vicinity of the site (see FSAR Figure 2.5.2-213). For this reason, Test Area 2 (shown in FSAR Figure 2.5.2-209) was drawn to compare rates of historical seismicity in this region. Both Test Area 1 and Test Area 2 show that historical seismicity since 1985 indicate lower overall rates of earthquake occurrences.

Some of the EPRI sources are large background zones, and it could be hypothesized that, if rates of historical seismicity increased in distant parts of those zones, and if an EPRI team used a smoothing assumption that resulted in spatially uniform seismicity throughout the source, the increase in seismicity rate might translate into an increase in seismicity rates within 40 km of the site, which might then affect seismic hazard. The assumption of spatially uniform seismicity for background zones was given low or zero weight by 5 of the 6 EPRI teams, as indicated by the following summary of background zones in Texas:

EPRI team	Typical background zone	Weight on uniform seismicity
Bechtel	BZ1, BZ2, BZ3	0.33
Dames & Moore	67, 20	0.0
Law	119, 124, 126	1.0
Rondout	50, 51	0.0
Weston	107, 109	0.2
Woodward-Clyde	local background	0.0

Thus the assumption of spatially uniform seismicity in background zones was not given high weight by 5 of the 6 EPRI teams. However, to test the above hypothesis, a third area (designated here Test Area 3) was defined as the rectangle comprising the limit of updated seismicity, i.e. 28°-38°N latitude and 93°-104°W longitude (see FSAR Figure 2.5.2-213). The same comparison was made for Test Area 3 as for the other two test areas, i.e. the overall rate of seismicity was calculated for the original EPRI earthquake catalog and for the catalog extended through 2006. Figure 2.5.2-3A (attached) shows the comparison of seismicity rates for the two catalogs. The conclusion is the same as for Test Areas 1 and 2, that is, the seismicity between 1985-2006 indicates, if anything, that seismicity rates have decreased. There is no reason to believe that any specific geometry of a large background zone for an EPRI team would lead to a different conclusion because no region of the Midwestern US has been recognized to have increased levels of naturally occurring earthquakes in the past 25 years. Further, if some region distant to the site had increased seismicity, the slightly decreased seismicity in Test Area 3 (as shown in Figure 2.5.2-3A) would buffer that increase, resulting in little or no change to average seismicity rates. Considering all of these factors, it is appropriate to use the seismicity rates for EPRI team sources as derived in the EPRI study (FSAR Reference 2.5-370).

Impact on R-COLA

None.

Impact on S-COLA

None.

Impact on DCD

None.

Attachment

Figure 2.5.2-3A - Comparison of Seismicity Rates for Test Area 3

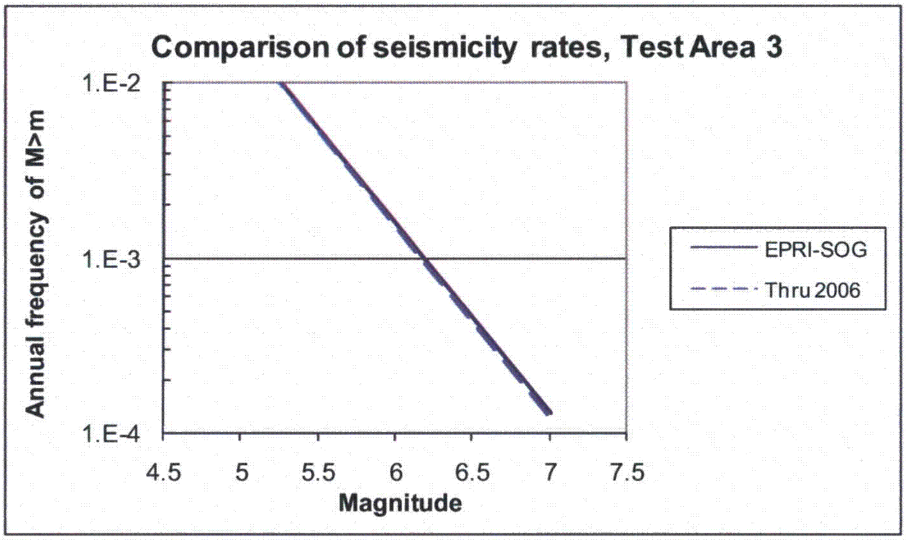

Figure 2.5.2-3A. Comparison of seismicity rates for Test Area 3, which is the rectangle defined by 28°—38°N latitude and 93°—104°W longitude, for the EPRI-SOG earthquake catalog and for the EPRI-SOG catalog updated through 2006.

Attachment 2

Response to Request for Additional Information No. 2929 (CP RAI #22)

RESPONSE TO REQUEST FOR ADDITIONAL INFORMATION

Comanche Peak, Units 3 and 4

Luminant Generation Company LLC

Docket Nos. 52-034 and 52-035

RAI NO.: 2929 (CP RAI #22)

SRP SECTION: 02.05.04 - Stability of Subsurface Materials and Foundations

QUESTIONS for Geosciences and Geotechnical Engineering Branch 1 (RGS1)

DATE OF RAI ISSUE: 7/17/2009

QUESTION NO.: 02.05.04-1

The Comanche Peak Units 3 and 4 (CPNPP) Final Safety Analysis Report (FSAR), in Section 2.5.4 (for example pages 121 and 129), states that the site "conforms to a relatively uniform site condition." The laboratory data obtained for samples tested from immediately beneath and to the sides of the power block structures, indicates potentially significant variability in properties (see, for example, Figures 2.5.4-219 and onward, data ranges described in Sections 2.5.4.2.3.1.1 and 2.5.4.2.3.3). Please provide the criteria used to make the judgment that the proposed site "conforms to a relatively uniform site condition[,]" and indicate if the assessment is appropriate for both site response and soil-structure interaction (SSI) assessments for which specific uniformity criteria are assumed.

ANSWER:

The uniformity of subsurface conditions, as described in FSAR Section 2.5.4.2, refers to the lateral continuity of geologic strata noted in the exploration borings, review of the Units 1 and 2 exploration data and construction photography, as well as regional exposures of strata surrounding the site. These units of limestone, shale and sandstones are characterized as nearly horizontal strata of relatively uniform thickness extending laterally across the CPNPP Units 3 and 4 project site that can be categorized by material properties that differ from the layer above or below.

The category I structures are to be founded directly on engineering Layer C which is characterized as a 60-ft thick limestone with a mean shear wave velocity of about 5800 feet/sec. Lying above Layer C are Layers A and B which will be excavated/removed. The uniformity of Layer C has been determined from the review of more than 150 geotechnical core borings drilled beneath the CPNPP Units 3 and 4 including a re-evaluation of the boring logs and lithologic descriptions, geophysical measurements and laboratory test results.

Review of Core Lithologic Descriptions and Photographs

The vertical and lateral distribution of shale within Layer C was quantified from a detailed review of each boring log to asses both the total cumulative percentage of shale as well as the lateral continuity of shale layers between borings. During the review of the core boring descriptions and photographs, four specific characteristics of intervals described as "shale" were noted, two of which are fine grained limestone (wackestone/packstone and micrite) that visually resembles shale yet has a more cemented characteristics as opposed to actual shale. However, for the purpose of this evaluation, each interval described as "shale" within the boring logs is included for conservatism.

Characteristics of Noted "Shale" in Layer C:

- *Shale* – indicated as having little to no reaction with HCl and signs of dessication upon drying or parting along laminae (Figure 2.5.4-1-1).
- *Laminated Shale/Limestone* - typically has a slight to strong reaction to HCl due to the presence of limestone and thinly, <0.1ft, to thicker, >0.2ft laminations of shale and/or silt (Figure 2.5.4-1-2).
- *Wackestone/Packstone* in Matrix- clasts of limestone in a fine grained matrix (Figure 2.5.4-1-3).
- *Micrite* – a fine grained limestone showing a strong to violent reaction to HCl (Figure 2.5.4-1-4).

Vertical and Lateral Evaluation of Layer C Uniformity

An extensive review of 114 geotechnical core boring logs was performed to compile each interval of shale for thickness, elevation and lithology. As described above, irrespective of the actual lithology noted, each "shale" layer was included in the following evaluation for conservatism. Specifically for Layer C, a total of 112.5 feet of "shale" was compared to 9455.9 total feet of limestone. The total percentage calculated from the total cored interval divided by the cumulative total of "shale" within Layer C is approximately 1.2 percent. As shown on Figures 2.5.4-1-5 and 2.5.4-1-6, the cumulative thickness (ft) of all shale layers for each boring are projected to a common latitudinal and longitudinal profile showing the CPNPP reactor building approximate centerlines. With the exception of boring B-2002, which has a total of almost 11 cummulative feet of shale (no actual shale as opposed to micrite or laminated limestone), the mean cumulative shale for all borings is less than 2 feet (1.2 percent) of Layer C (see Table 2.5.4.1-1).

The potential presence of laterally continuous shale layers was evaluated by plotting the thickness of shale within each boring at the respective elevation as shown on Figures 2.5.4-1-7 and 2.5.4-1-8. Four shale horizons (CS1, CS2, CS3 and CS4) were identified and are shown on Figures 2.5.4-1-7 and 2.5.4-1-8. Also note in Figure 2.5.4-1-7 that the interface between the overlying Layer B2 and Layer C beneath the Unit 4 indicates limited zones of shale in the range of elevation 782 which is the estimated mean average top elevation of Layer C. Subsection 2.5.4.12.4 provides a commitment that top of foundation inspections will identify shale pockets for removal prior to placement of fill or structural concrete thus this horizon was not included in the following evaluation although the occurrence of shale was included in cumulative thickness and percentage estimates.

- Horizon CS1 Ranges from about Elevation 766-763 and includes shale thicknesses from 0.2 to 1.5 ft thick.
- Horizon CS2 Ranges from about Elevation 749-746 and includes shale thicknesses from 0.2 to 1.9 ft thick.
- Horizon CS3 Ranges from about Elevation 745-742 and includes shale thicknesses from 0.2 to 2.6 ft thick.

- Horizon CS4 Ranges from about Elevation 736-733 and includes shale thicknesses from 0.3 to 1.8 ft thick.

Each of these 4 shale horizons were plotted in plan view to determine the lateral extent, as shown on Figures 2.5.4-1-9, 2.5.4-1-10, 2.5.4-1-11 and 2.5.4-1-12. Only Figures 2.5.4-1-11 and 2.5.4-1-12 indicate a zone of shale in borings B-1030 (Horizon CS4), B-1005, B-1001-I, B-1010, B-1013, and B-1016 that can be mapped laterally. These shale beds were identified under the western portion of Unit 4 and cannot be continuously mapped across the site.

Uniformity of Geophysical Measurements

Resistivity measurements were used to evaluate the potential shale content within Layer C. The 15 borings with resistivity measurements were evaluated by using data from Layer D, a continuous shale layer beneath Layer C as a known baseline. Layer D has an average Single Point Resistance, (SPR) of approximately 12 to 16 Ohm. Within Layer C SPR varies from 28 to 80 Ohm. To further evaluate the resistivity measurements sensitivity to shale within Layer C, known intervals of shale were identified, such as elevations 750.9 and 748.3 in Boring Log B-1000. The resistivity measurements from this interval range from 32-50 and 35-45 Ohm's respectively, which is generally higher than typical shale values

Laboratory Measurements

Shear wave velocity was measured for a number of rock core samples (FSAR Figure 2.5.4-238) as part of the laboratory testing program. Because laboratory tests are performed on relatively small (2.5-inch diameter) intact specimens, the effects of weathering, fissures, and discontinuities of the larger rock mass typically are not reflected in the results. Generally, laboratory-measured shear wave velocities are higher than those measured in the field because the small lab samples lack the rock-mass discontinuities present in the field, as reflected by the data obtained for this site. For these reasons, the results of the laboratory shear wave velocity measurements do not provide a good representation of the subsurface mass properties. Consequently they were only used as an indicator of the degree of weathering and soundness of the rock specimens and not used for formulating the site shear wave velocity model.

Summary of Layer C Uniformity

A thorough evaluation of the core lithologic descriptions, photographs and geophysical measurements determined that shale is mostly limited to isolated pockets and is not in continuous layers within Layer C. Further, the total percentage of "shale" does not constitute a reduction in the mass properties of Layer C.

The SSI analyses use of horizontal uniformity is discussed in the response to Question 02.05.04-2 of RAI No. 2929 (CP RAI #22). The site-specific SSI analyses addressed in Section 3.7 and Appendices 3KK, 3LL, 3MM, and 3NN do not assume uniformity in the vertical direction, but consider layered site with input engineering properties based on filed measurements. Variations of the subgrade properties are considered as presented in Chapter 2, specifically Table 2.5.2-227. The SSI analyses consideration of the variation of engineering properties of the stratigraphy in the vertical direction is discussed further in the responses to Questions 02.05.04-4 and 02.05.04-9 of RAI No. 2929 (CP RAI #22).

<u>Impact on R-COLA</u>

None.

Impact on S-COLA

None.

Impact on DCD

None.

Attachments

Table 2.5.4.1-1 - Compilation of Shale Percentage in Layer C (13 sheets)

Figure 2.5.4-1-1 – Shale Description from Boring Log Data Report

Figure 2.5.4-1-2 – Laminated Shale/Limestone Description from Boring Log Data Report

Figure 2.5.4-1-3 – Wackestone/Packstone in Matrix Description from Boring Log Data Report

Figure 2.5.4-1-4 – Micrite Description from Boring Log Data Report

Figure 2.5.4-1-5 – Latitudinal Profile Showing Shale Thickness in Layer C

Figure 2.5.4-1-6 – Longitudinal Profile Showing Shale Thickness in Layer C

Figure 2.5.4-1-7 – Areas with Shale Beds at Various Locations within Layer C below Unit 4

Figure 2.5.4-1-8 – Areas with Shale Beds at Various Locations within Layer C below Unit 3

Figure 2.5.4-1-9 – Shale Beds within CS1 of Layer C

Figure 2.5.4-1-10 – Shale Beds within CS2 of Layer C

Figure 2.5.4-1-11 – Shale Beds within CS3 of Layer C

Figure 2.5.4-1-12 – Shale Beds within CS4 of Layer C

Table 2.5.4.1-1
Compilation of Shale Percentage in Layer C

Boring	B1000	B1001	B1002	B1003	B1003Off	B1004	B1005	B1006	B1007
Latitude	32.302089	32.302665	32.302155	32.301421	32.301421	32.301105	32.302099	32.301238	32.302483
Longitude	97.794947	97.795019	97.794461	97.794756	97.794756	97.795553	97.795441	97.794264	97.795007
Top of C (elevation)	784.008	781.984	782.863	783.488	783.570	782.404	782.018	781.921	783.823
Bottom of C (elevation)	718.008	716.784	717.063	717.588	717.670	717.204	717.018	716.521	718.223
Top and Bottom Elevation of Shale Interbeds	782.2	779.3		781.5			780.8	780.4	748.9
	781	778.5		780.9			780.6	780.1	748.5
	766	750.9					745	728.6	746.6
	764.5	749.8					743.1	727	744
		748.3					735.8		
		747					735		
							729.9		
							728		
Thickness (ft) of Shale Interbeds	1.2	0.8		0.6			0.2	0.3	0.4
	1.5	1.1					1.9	1.6	2.6
		1.3					0.8		
							1.9		
Total Thickness (ft) of Shale Per Boring Based on Boring Logs In Layer C	2.7	3.2	0	0.6	0	0	4.8	1.9	3
Percentage of Shale Based on Boring Logs in Layer C	4.09	4.91	0.00	0.91	0.00	0.00	7.38	2.91	4.57

Shale Lithology				
		Micrite		Laminated shale and limestone
		Shale		Wackestone/Packstone in matrix

RAI 2.5.4-1

Table 2.5.4.1-1
Compilation of Shale Percentage in Layer C

Boring	B1008	B1009I	B1010	B1011I	B1012	B1013	B1014	B1015	B1016
Latitude	32.302128	32.301783	32.301751	32.302052	32.302301	32.301566	32.302245	32.301635	32.301336
Longitude	97.794738	97.794886	97.795176	97.795222	97.793311	97.795231	97.795261	97.794689	97.795193
Top of C (elevation)	784.356	784.201	783.241	782.310	782.143	782.531	782.347	784.394	783.590
Bottom of C (elevation)	716.756	719.101	717.441	717.210	717.543	717.331	716.197	719.294	717.840
Top and Bottom Elevation of Shale Interbeds	765	781.9	781.3	780.3	780.2	781		782.1	781.6
	764.5	781.45	780	780	779.8	780.7		781.7	781.3
	764	737.9	765.7	744.8		745.1		777.1	744.7
	763.5	737.2	764.7	742.9		744.9		776.8	744.2
	763.1	731.6	745.4	735.9		744.7		774	736.8
	762.6	729.9	743.4	735.3		744.5		773.7	736.1
	760.6		736.5			736		766.2	
	760.2		735.5			735.5		765.9	
	759							759.3	
	758.6							757	
	756.2							750.1	
	755.9							749.9	
	754.4							725.6	
	752.95							724	
	751.5								
	750.6								
Thickness (ft) of Shale Interbeds	0.5	0.45	1.3	0.3	0.4	0.3		0.4	0.3
	0.5	0.7	1	1.9		0.2		0.3	0.5
	0.5	1.7	2	0.6		0.2		0.3	0.7
	0.4		1			0.5		0.3	
	0.4							2.3	
	0.3							0.2	
	1.45							1.6	
	0.9								
Total Thickness (ft) of Shale Per Boring Based on Boring Logs In Layer C	4.95	2.85	5.3	2.8	0.4	1.2	0	5.4	1.5
Percentage of Shale Based on Boring Logs in Layer C	7.32	4.38	8.05	4.30	0.62	1.84	0.00	8.29	2.28

Shale Lithology		
	Micrite	Laminated shale and limestone
	Shale	Wackestone/Packstone in matrix

RAI 2.5.4-1

Table 2.5.4.1-1
Compilation of Shale Percentage in Layer C

Boring	B1017	B1018	B1019	B1020	B1021	B1022	B1023	B1024	B1025
Latitude	32.300921	32.302559	32.302349	32.301865	32.302180	32.301738	32.301524	32.301583	32.301370
Longitude	97.795012	97.795427	97.795503	97.795649	97.794228	97.795396	97.795596	97.794983	97.794682
Top of C (elevation)	785.768	780.963	781.322	782.737	782.675	782.880	783.278	784.546	783.318
Bottom of C (elevation)	721.568	716.663	716.172	717.737	716.675	719.280	721.678		720.218
Top and Bottom Elevation of Shale Interbeds	783.7	766.4		781.1			781.3		745.3
	783.2	765.2		780.5			780.5		744.7
		757.5							
		757.2							
	761.9	748.3							
	761.4	747.4							
	754.8	726.4							
	753.1	726.1							
		723.4							
		723.1							
	738.5								
	737.8								
Thickness (ft) of Shale Interbeds	0.5	1.2		0.6			0.8		0.6
		0.3							
	0.5	0.9							
	1.7	0.3							
		0.3							
	0.7								
Total Thickness (ft) of Shale Per Boring Based on Boring Logs In Layer C	3.4	3	0	0.6	0	0	0.8	0	0.6
Percentage of Shale Based on Boring Logs in Layer C	5.30	4.67	0.00	0.92	0.00	0.00	1.30	0.00	0.95

Shale Lithology
- Micrite
- Shale
- Laminated shale and limestone
- Wackestone/Packstone in matrix

Table 2.5.4.1-1
Compilation of Shale Percentage in Layer C

Boring	B1026	B1027	B1028	B1029	B1030	B1031	B1032	B1034	B1035
Latitude	32.301182	32.300953	32.302768	32.302294	32.302152	32.301728	32.301367	32.300752	32.300773
Longitude	97.794894	97.794598	97.795057	97.794972	97.795721	97.795699	97.795430	97.794931	97.794390
Top of C (elevation)	785.732	786.019	784.764	781.878	782.875	784.713	784.317	785.963	785.806
Bottom of C (elevation)	754.300	720.219	766.500	715.978	717.775	763.600	766.800	720.463	756.100
Top and Bottom Elevation of Shale Interbeds		748.3	780.65		781	782.5	782.9		783.8
		746.4	779.1		780.6	782.1	782.1		783.5
		739			736.1		775.4		783.1
		738.4			735.3		774.7		781.8
Thickness (ft) of Shale Interbeds		1.9	1.55		0.4	0.4	0.8		0.3
		0.6			0.8		0.7		1.3
Total Thickness (ft) of Shale Per Boring Based on Boring Logs In Layer C	0	2.5	1.55	0	1.2	0.4	1.5	0	1.6
Percentage of Shale Based on Boring Logs in Layer C	0.00	3.80	8.49	0.00	1.84	1.89	8.56	0.00	5.39

Shale Lithology				
	(red)	Micrite	(green)	Laminated shale and limestone
	(blue)	Shale	(yellow)	Wackestone/Packstone in matrix

RAI 2.5.4-1

Table 2.5.4.1-1
Compilation of Shale Percentage in Layer C

Boring	B1036	B1037	B1038	B1039	B1040	B1041	B1042	B1043	B1044
Latitude	32.301321	32.301714	32.302542	32.301798	32.301908	32.302024	32.301746	32.303049	32.303130
Longitude	97.794467	97.794522	97.794685	97.794260	97.794373	97.794205	97.794151	97.796126	97.795313
Top of C (elevation)	784.847	784.036	782.825	783.196	783.442	782.695	781.111	784.114	782.706
Bottom of C (elevation)	783.650	718.136	717.725	772.100	746.550	717.095	717.711	747.700	762.500
Top and Bottom Elevation of Shale Interbeds		781.6	782.1	782.8	781.5	780.5	771.9	782.1	780.8
		781.300	781.9	782.4	781.1	780.3	771.4	781.6	780.5
							749.1		769.8
							748.9		769.1
			736.3						764.8
			735.6						764.1
Thickness (ft) of Shale Interbeds		0.3	0.2	0.4	0.4	0.2	0.5	0.5	0.3
							0.2		0.7
			0.7						0.7
Total Thickness (ft) of Shale Per Boring Based on Boring Logs In Layer C	0	0.3	0.9	0.4	0.4	0.2	0.7	0.5	1.7
Percentage of Shale Based on Boring Logs in Layer C	0.00	0.46	1.38	3.60	1.08	0.30	1.10	1.37	8.41

Shale Lithology		
	Micrite	Laminated shale and limestone
	Shale	Wackestone/Packstone in matrix

RAI 2.5.4-1

Table 2.5.4.1-1
Compilation of Shale Percentage in Layer C

Boring	B1045	B1047	B1048	B1049	B1050	B1051	B1052	B1053	B1054
Latitude	32.303182	32.302903	32.302964	32.303023	32.303073	32.302685	32.302808	32.302828	32.302928
Longitude	97.795127	97.795900	97.795514	97.794915	97.794519	97.796078	97.795275	97.795080	97.794285
Top of C (elevation)	783.565	780.510	782.482	783.814	782.704	782.690	781.912	778.654	783.063
Bottom of C (elevation)	762.400	716.910		740.400	717.104				764.2
Top and Bottom Elevation of Shale Interbeds	765.5			781.6	781				781.1
	764.8			781.1	780.3				780.1
				768.6	743.5				764.55
				766.4	743.2				764.2
				745.4	735.8				
				745	735.1				
				744.4					
				744					
Thickness (ft) of Shale Interbeds	0.7			0.5	0.7				1
				2.2	0.3				0.35
				0.4	0.7				
				0.4					
Total Thickness (ft) of Shale Per Boring Based on Boring Logs In Layer C	0.7	0	0	3.5	1.7	0	0	0	1.35
Percentage of Shale Based on Boring Logs in Layer C	3.31	0.00	0.00	8.06	2.59	0.00	0.00	0.00	7.16

Shale Lithology		
	Micrite (red)	Laminated shale and limestone (green)
	Shale (blue)	Wackestone/Packstone in matrix (yellow)

Table 2.5.4.1-1
Compilation of Shale Percentage in Layer C

Boring	B1063	B1064	B2000	B2001	B2002	B2003	B2003Off	B2004	B2005
Latitude	32.303493	32.303177	32.302496	32.303059	32.302558	32.301863	32.301863	32.302428	32.302495
Longitude	97.793597	97.793548	97.791688	97.791768	97.791214	97.791578	97.791578	97.792297	97.792190
Top of C (elevation)	784.955	783.246	779.427	780.886	779.413	779.988	781.040	782.128	781.523
Bottom of C (elevation)	737.2	738.55	715.227	716.886	716.313	715.788	716.840	716.928	716.523
Top and Bottom Elevation of Shale Interbeds	781.65	781.1	733.55	778.6	762.2	748		758.55	743.3
	778.5	780.55	733	778.2	761.2	747.5		757.05	742.7
	769.8				758.8	747			
	768.4				755.2	746.5			
	746.8				750	745.5			
	746				749.2	744.7			
	738.55				748.3	744			
	737.9				747.200	743.4			
					745.5	743			
					744.800	742.2			
					735	735			
					733.200	733.2			
					728.8				
					727.500				
Thickness (ft) of Shale Interbeds	3.15	0.55	0.55	0.4	1	0.5		1.5	0.6
	1.4				3.6	0.5			
	0.8				0.8	0.8			
	0.65				1.1	0.6			
					0.7	0.8			
					1.8	1.8			
					1.3				
Total Thickness (ft) of Shale Per Boring Based on Boring Logs In Layer C	6	0.55	0.55	0.4	10.3	5	0	1.5	0.6
Percentage of Shale Based on Boring Logs in Layer C	12.56	1.23	0.86	0.62	16.32	7.79	0.00	2.30	0.92

Shale Lithology

(red)	Micrite	(green)	Laminated shale and limestone
(blue)	Shale	(yellow)	Wackestone/Packstone in matrix

RAI 2.5.4-1

Table 2.5.4.1-1
Compilation of Shale Percentage in Layer C

Boring	B2006	B2007	B2008	B2009I	B2010	B2011I	B2012	B2013	B2014
Latitude	32.302839	32.302887	32.302559	32.302178	32.302148	32.302447	32.301958	32.302651	32.302029
Longitude	97.792027	97.791742	97.791428	97.791619	97.791903	97.791986	97.791983	97.792012	97.791436
Top of C (elevation)	781.094	780.731	780.124	779.774	780.208	781.782	781.392	781.955	779.707
Bottom of C (elevation)	716.394	716.531	715.924	716.174	715.508	717.282	717.192	716.955	714.707
Top and Bottom Elevation of Shale Interbeds	779.5	778.5		727.5		779.2			
	778.9	777.9		726.2		778.8			
	743.8					728.9			
	741.8					726			
Thickness (ft) of Shale Interbeds	0.6	0.6		1.3		0.4			
	2					2.9			
Total Thickness (ft) of Shale Per Boring Based on Boring Logs In Layer C	2.6	0.6	0	1.3	0	3.3	0	0	0
Percentage of Shale Based on Boring Logs in Layer C	4.02	0.93	0.00	2.04	0.00	5.12	0.00	0.00	0.00

Shale Lithology		
	Micrite (red)	Laminated shale and limestone (green)
	Shale (blue)	Wackestone/Packstone in matrix (yellow)

RAI 2.5.4-1

Table 2.5.4.1-1
Compilation of Shale Percentage in Layer C

Boring	B2015	B2016	B2017	B2018Off	B2019	B2020	B2021	B2022	B2023
Latitude	32.301730	32.301289	32.302970	32.302742	32.302253	32.302576	32.302127	32.301914	32.301985
Longitude	97.791945	97.791745	97.792191	97.792256	97.792403	97.790951	97.792148	97.792345	97.791705
Top of C (elevation)	782.279	779.240	782.367	783.070	782.874	781.148	782.761	784.079	780.151
Bottom of C (elevation)	717.079	715.440	716.767	717.970	717.574	716.048	719.161	718.179	733.500
Top and Bottom Elevation of Shale Interbeds	735.5		779.9			778.8	780	736.1	
	734.7		779.6			778.4	779.8	735.5	
			752.1			749.1			
			751.8			748.8			
			748.2						
			747.3						
Thickness (ft) of Shale Interbeds	0.8		0.3			0.4	0.2	0.6	
			0.3			0.3			
			0.9						
Total Thickness (ft) of Shale Per Boring Based on Boring Logs In Layer C	0.8	0	1.5	0	0	0.7	0.2	0.6	0
Percentage of Shale Based on Boring Logs in Layer C	1.23	0.00	2.29	0.00	0.00	1.08	0.31	0.91	0.00

Shale Lithology

- Micrite
- Shale
- Laminated shale and limestone
- Wackestone/Packstone in matrix

RAI 2.5.4-1

Table 2.5.4.1-1
Compilation of Shale Percentage in Layer C

Boring	B2024	B2025	B2026	B2027	B2028	B2029	B2030	B2031	B2032
Latitude	32.301735	32.301594	32.301334	32.302296	32.301824	32.302693	32.302578	32.302127	32.301719
Longitude	97.791505	97.791648	97.791350	97.790650	97.790568	97.791724	97.792593	97.792445	97.792373
Top of C (elevation)	781.053	780.231	779.993	779.598	776.536	780.578	782.952	783.043	783.291
Bottom of C (elevation)	716.953	730.150	715.793	752.000	748.250	716.678	717.452	753.100	753.000
Top and Bottom Elevation of Shale Interbeds			771.200			778.5	735.8		765.5
			770.000			778.2	735.2		765.3
Thickness (ft) of Shale Interbeds			1.2			0.3	0.6		0.2
Total Thickness (ft) of Shale Per Boring Based on Boring Logs In Layer C	0	0	1.2	0	0	0.3	0.6	0	0.2
Percentage of Shale Based on Boring Logs in Layer C	0.00	0.00	1.87	0.00	0.00	0.47	0.92	0.00	0.66

Shale Lithology			
	Micrite		Laminated shale and limestone
	Shale		Wackestone/Packstone in matrix

RAI 2.5.4-1

Table 2.5.4.1-1
Compilation of Shale Percentage in Layer C

Boring	B2033	B2034	B2035	B2036	B2037	B2038	B2039	B2040	B2041
Latitude	32.301743	32.301100	32.301172	32.301710	32.302100	32.302936	32.302142	32.302318	32.302419
Longitude	97.792183	97.791674	97.791112	97.791208	97.791275	97.791427	97.791074	97.791126	97.790952
Top of C (elevation)	782.788	779.816	778.716	779.853	777.888	781.153	777.688	779.436	779.814
Bottom of C (elevation)	774.700	715.416	729.600	757.350	713.288	716.653	757.500	735.700	714.964
Top and Bottom Elevation of Shale Interbeds								777.2	
								776.6	
Thickness (ft) of Shale Interbeds								0.6	
Total Thickness (ft) of Shale Per Boring Based on Boring Logs In Layer C	0	0	0	0	0	0	0	0.6	0
Percentage of Shale Based on Boring Logs in Layer C	0.00	0.00	0.00	0.00	0.00	0.00	0.00	1.37	0.00

Shale Lithology		
	Micrite	Laminated shale and limestone
	Shale	Wackestone/Packstone in matrix

Table 2.5.4.1-1
Compilation of Shale Percentage in Layer C

Boring	B2042	B2044	B2045	B2046	B2047	B2048	B2049	B2050	B2051
Latitude	32.302143	32.303442	32.303538	32.303568	32.303678	32.303307	32.303350	32.303387	32.303469
Longitude	97.790905	97.792878	97.792088	97.791893	97.791102	97.792661	97.792264	97.791670	97.791259
Top of C (elevation)	778.847	782.160	783.030	781.368	780.396	783.281	782.864	781.553	780.866
Bottom of C (elevation)	740.800	768.750	757.300	753.500	718.800	717.081	738.600	727.300	715.866
Top and Bottom Elevation of Shale Interbeds				779.2		735.5	780.8		778.8
				778.7		735.2	780.2		778.2
Thickness (ft) of Shale Interbeds				0.5		0.3	0.6		0.6
Total Thickness (ft) of Shale Per Boring Based on Boring Logs In Layer C	0	0	0	0.5	0	0.3	0.6	0	0.6
Percentage of Shale Based on Boring Logs in Layer C	0.00	0.00	0.00	1.79	0.00	0.45	1.36	0.00	0.92

Shale Lithology		
	Micrite	Laminated shale and limestone
	Shale	Wackestone/Packstone in matrix

RAI 2.5.4-1

Table 2.5.4.1-1
Compilation of Shale Percentage in Layer C

Boring	B2052	B2053	B2054	B2055	B2059	B2063
Latitude	32.303105	32.303175	32.303228	32.303323	32.302470	32.301973
Longitude	97.792826	97.792026	97.791835	97.791028	97.790926	97.790846
Top of C (elevation)	783.070	782.095	782.035	780.946	783.125	779.146
Bottom of C (elevation)	771.600	764.100	759.500	740.200	781.800	778.100
Top and Bottom Elevation of Shale Interbeds	773.9					
	773.3					
	781					
	780.6					
Thickness (ft) of Shale Interbeds	0.6					
	0.4					
Total Thickness (ft) of Shale Per Boring Based on Boring Logs In Layer C	1	0	0	0	0	0
Percentage of Shale Based on Boring Logs in Layer C	8.72	0.00	0.00	0.00	0.00	0.00

Shale Lithology	(red)	Micrite	(green)	Laminated shale and limestone
	(blue)	Shale	(yellow)	Wackestone/Packstone in matrix

RAI 2.5.4-1

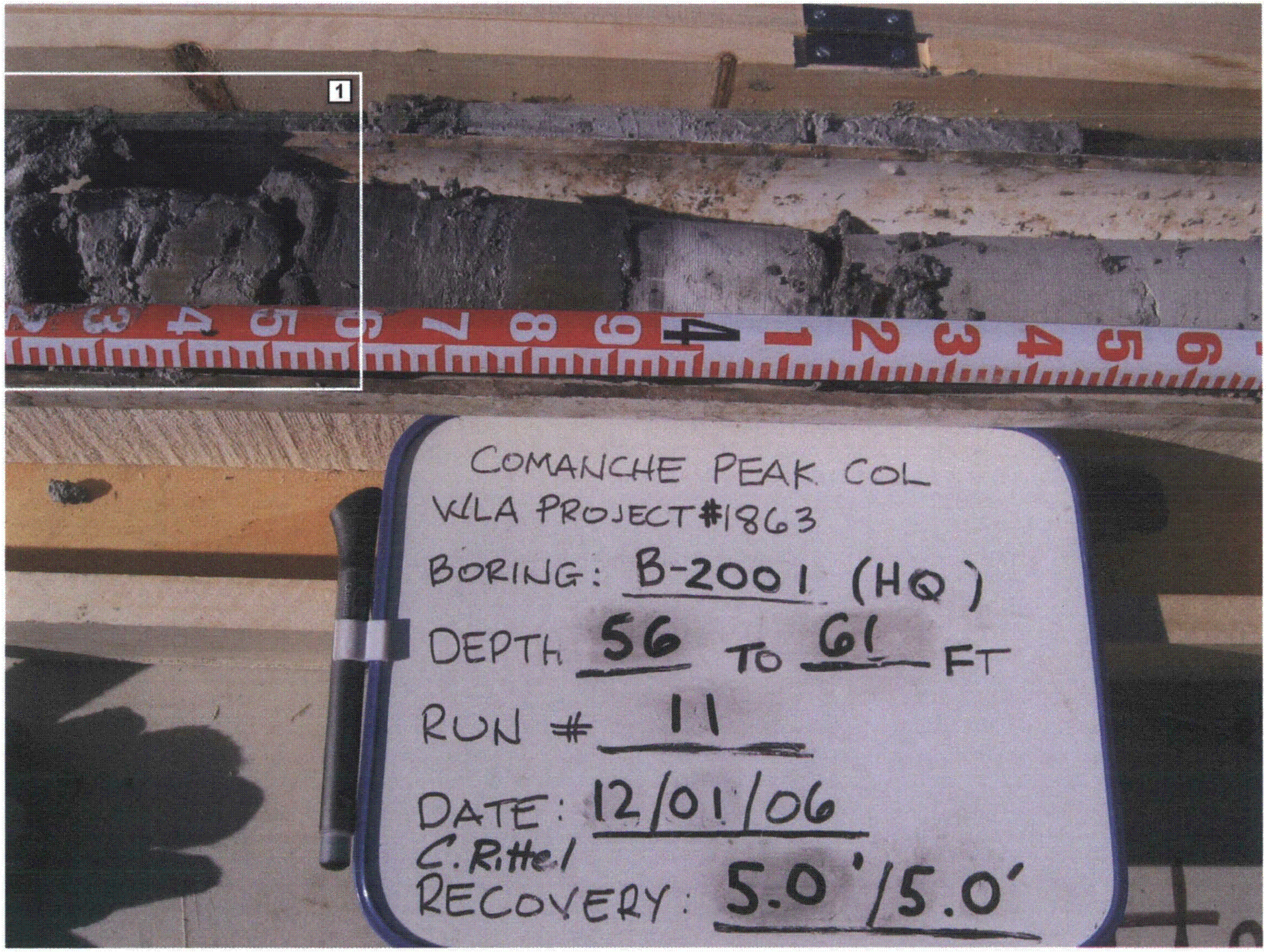

Description from Boring Log Data Report, Rev. 0:
- Boring: B-2001
- Depth: 778.6 to 778.2

1 Shale: mudstone; medium dark gray (N4); slightly weathered (SW); very weak to extremely weak (R1-R0); slight HCl reaction; disturbance from sampling

COMANCHE PEAK NUCLEAR POWER PLANT
UNITS 3 AND 4

Shale
FIGURE 2.5.4-1-1

Rev 0

Laminated Shale/Limestone
FIGURE 2.5.4-1-2

Rev 0

COMANCHE PEAK NUCLEAR POWER PLANT
UNITS 3 AND 4

Description from Boring Log Data Report, Rev. 0:

- Boring: B-1027
- Depth: 748.3 ft to 746.4 ft

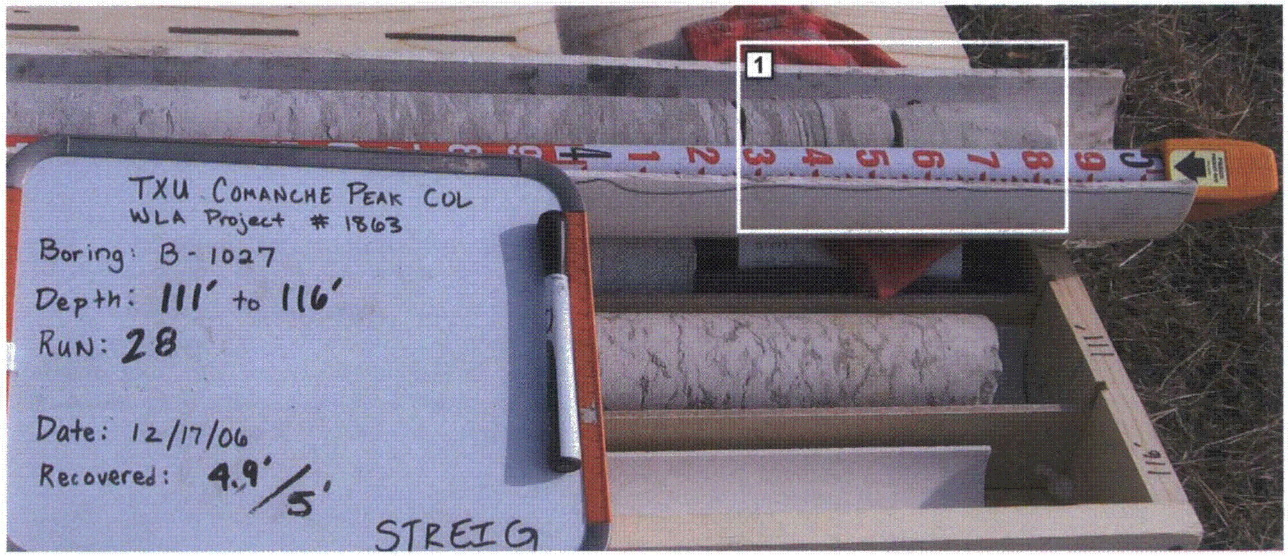

[1] Shale (lamintaed shale/limetsone): mudstone; calcareous shale; fine grained; slightly weathered (SW); weak (R2); massive to strongly laminated; slight HCl reaction

Description from Boring Log Data Report, Rev. 0:
- Boring: B-2003
- Depth: 735 ft to 733.2 ft

1 Shale (wackestone/packstone in matrix: fresh; very weak (R1); common rip-up clasts; trace fossils

COMANCHE PEAK NUCLEAR POWER PLANT
UNITS 3 AND 4

Wackestone/Packstone in Matrix
FIGURE 2.5.4-1-3

Rev 0

COMANCHE PEAK NUCLEAR POWER PLANT
UNITS 3 AND 4

Rev 0

Micrite
FIGURE 2.5.4-1-4

Description from Boring Log Data Report, Rev. 0:
- Boring: B-2011-I
- Depth: 728.9 ft to 726 ft

1 Shale: calcareous; light olive gray; very fine grained and massive to weakly bedded; fresh to slightly weathered (F-SW) weak (R2); burrows

COMANCHE PEAK NUCLEAR POWER PLANT
UNITS 3 AND 4

Latitudinal Profile Showing Shale Thickness in Layer C

FIGURE 2.5.4-1-5 Rev 0

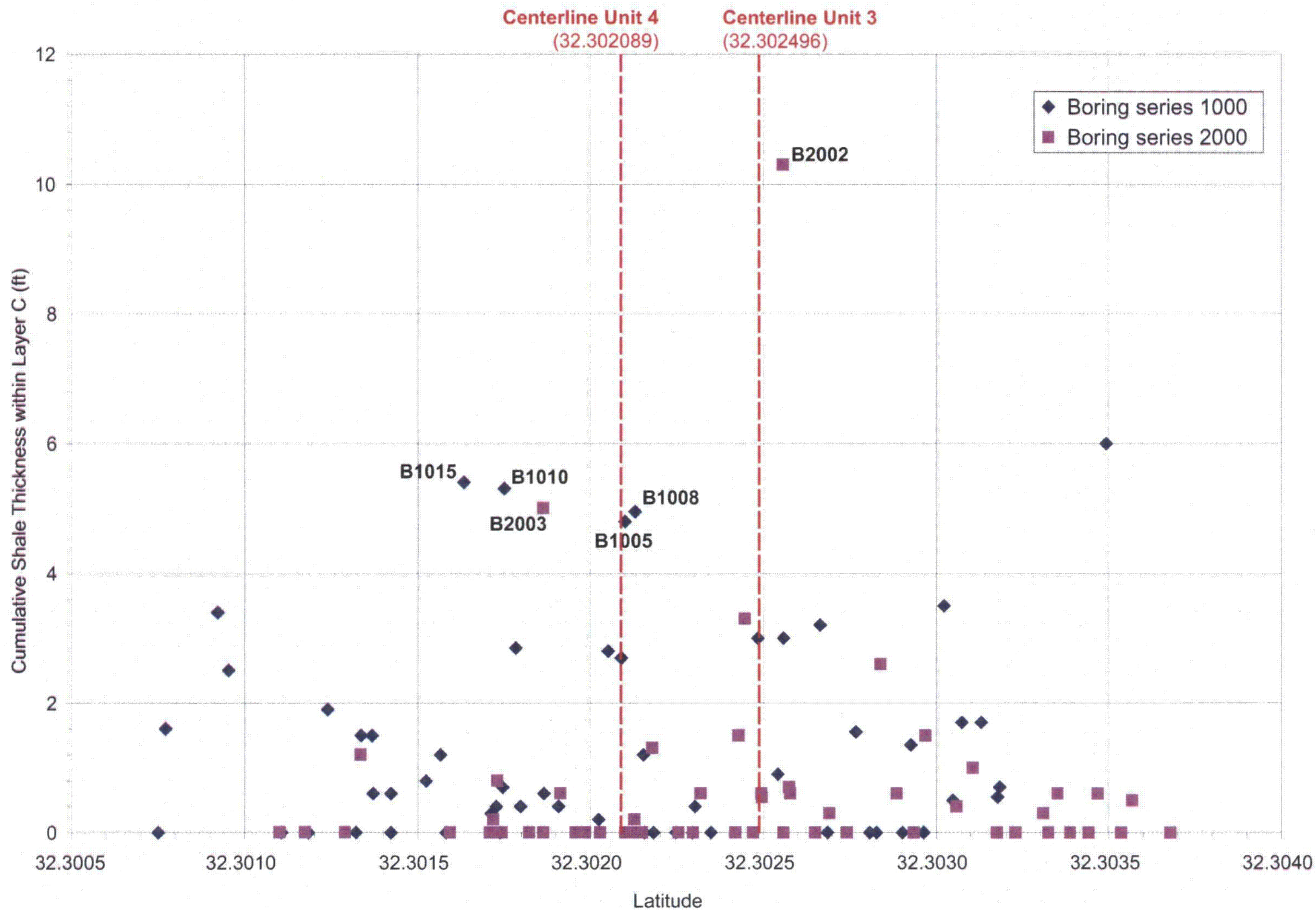

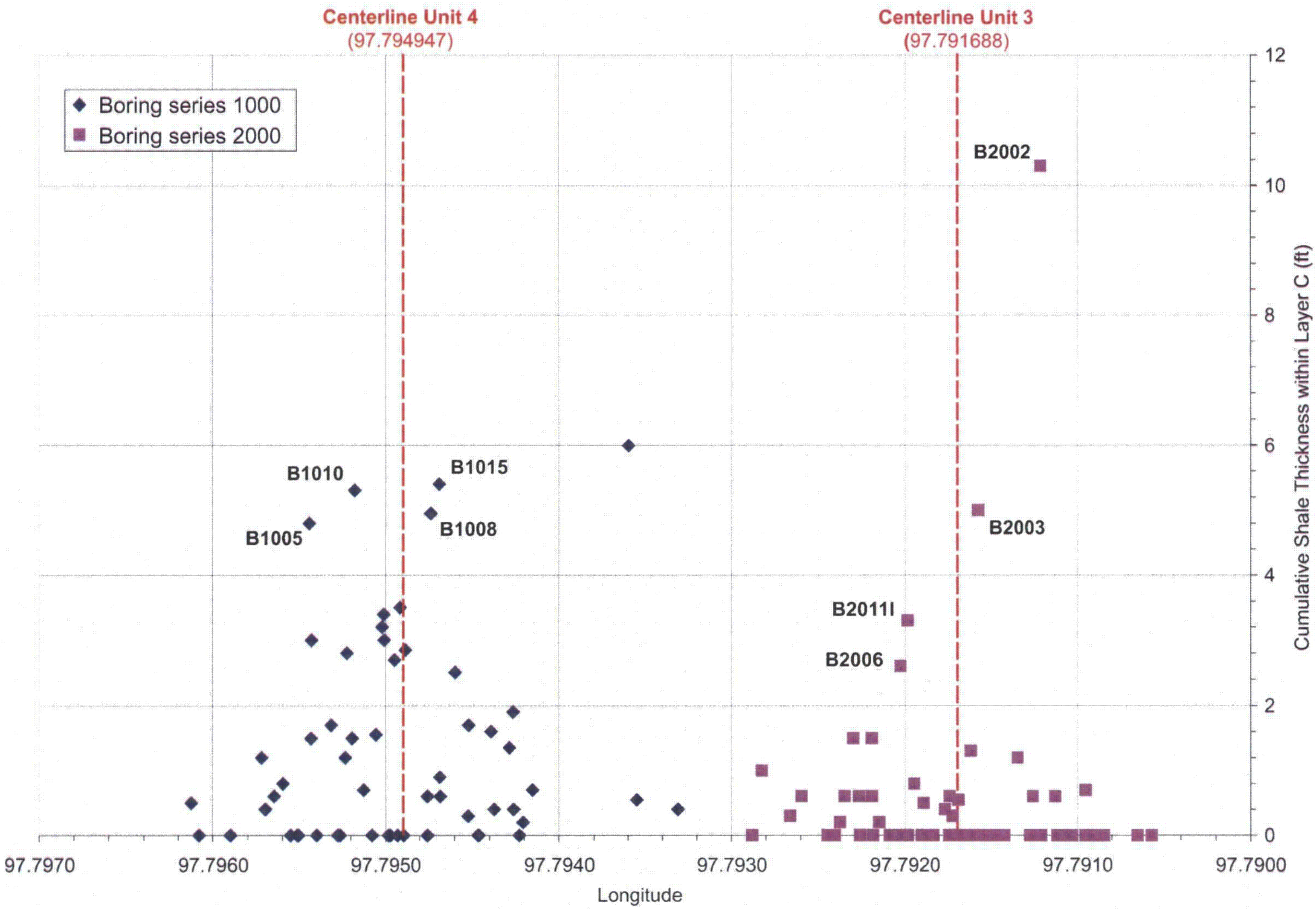

COMANCHE PEAK NUCLEAR POWER PLANT
UNITS 3 AND 4

Longitudinal Profile Showing Shale Thickness in Layer C
FIGURE 2.5.4-1-6
Rev 0

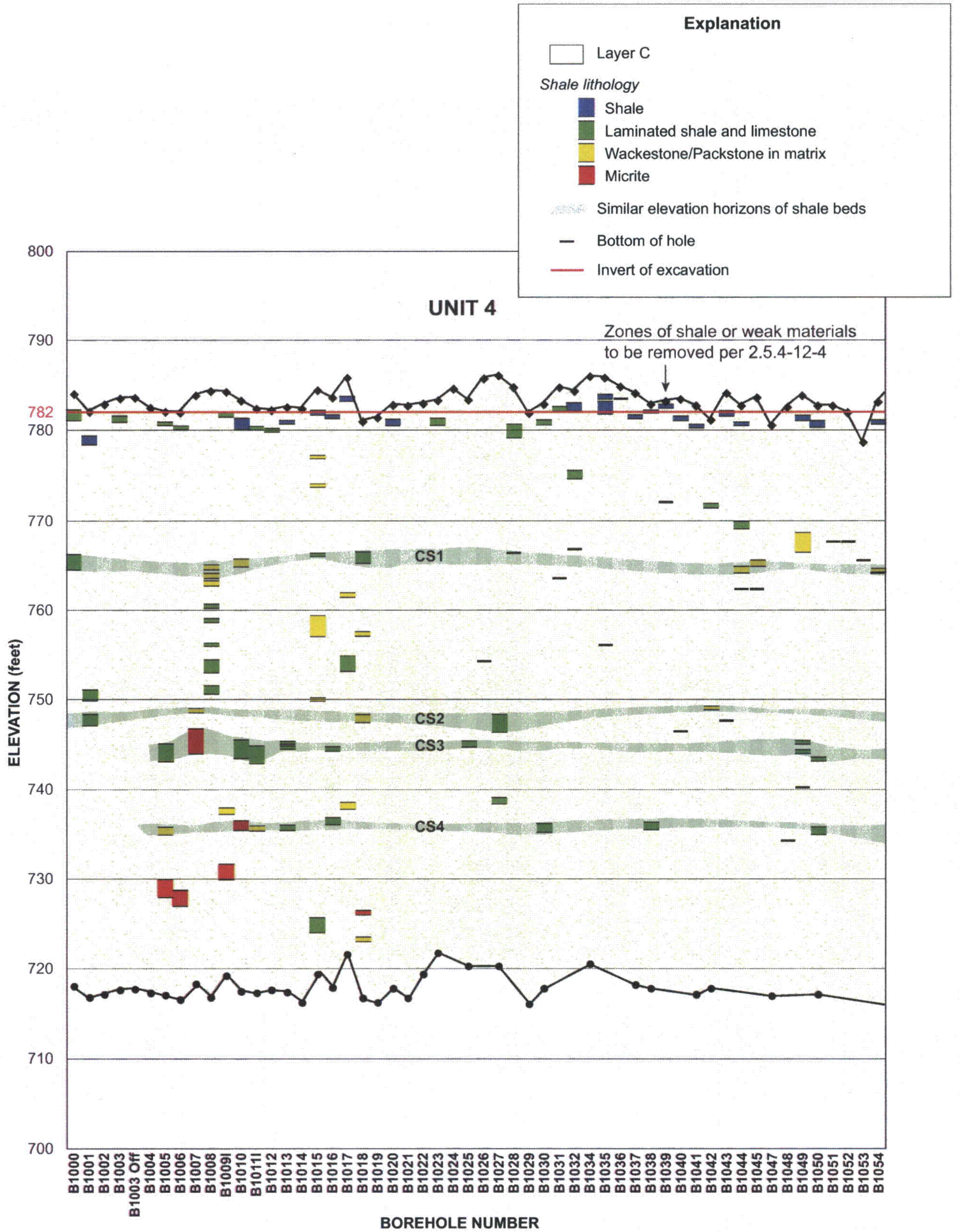

Areas with Shale Beds at Various Locations within Layer C below Unit 4 FIGURE 2.5.4-1-7 Rev 0	COMANCHE PEAK NUCLEAR POWER PLANT UNITS 3 AND 4

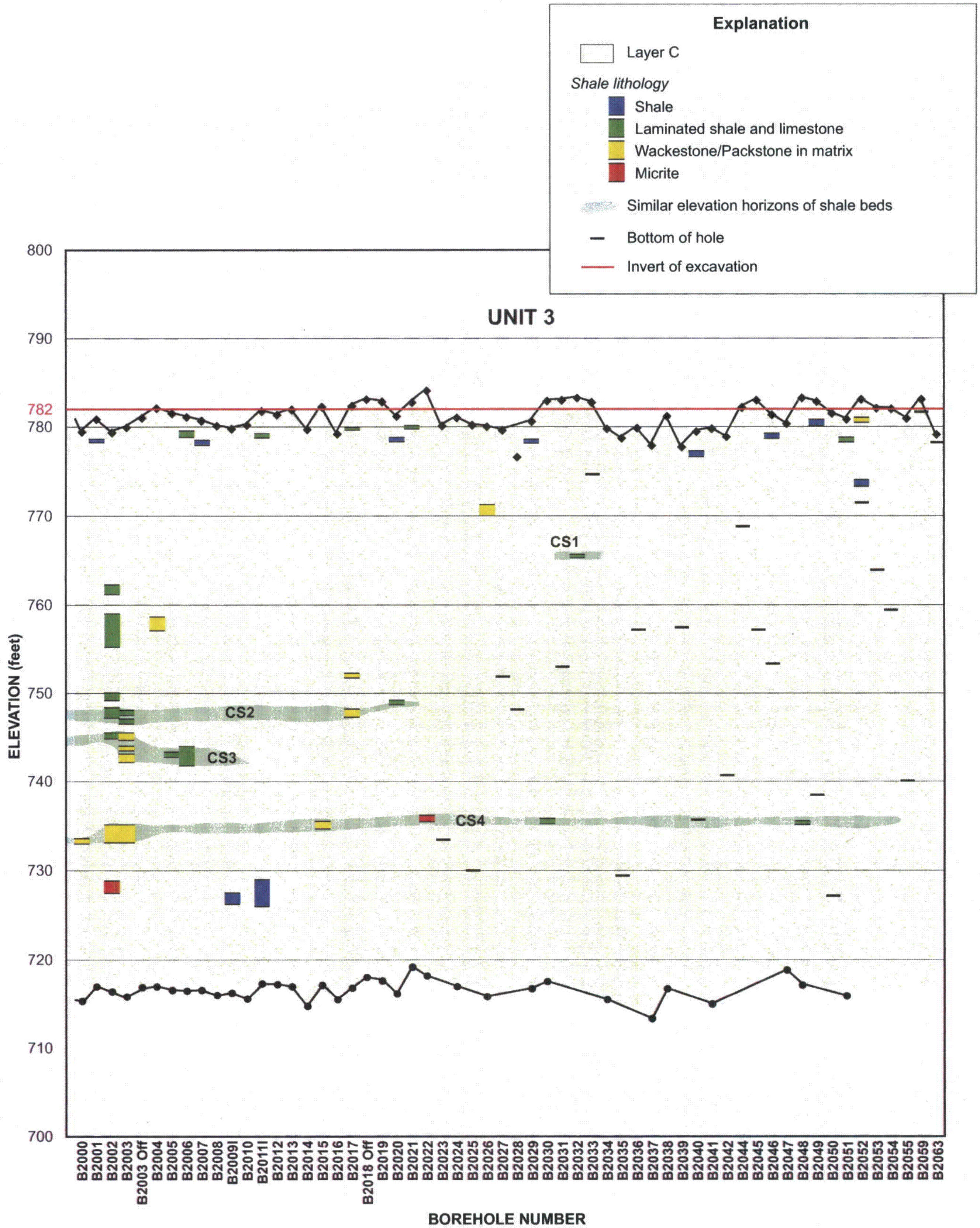

Areas with Shale Beds at Various Locations within Layer C below Unit 3 FIGURE 2.5.4-1-8 Rev 0	COMANCHE PEAK NUCLEAR POWER PLANT UNITS 3 AND 4

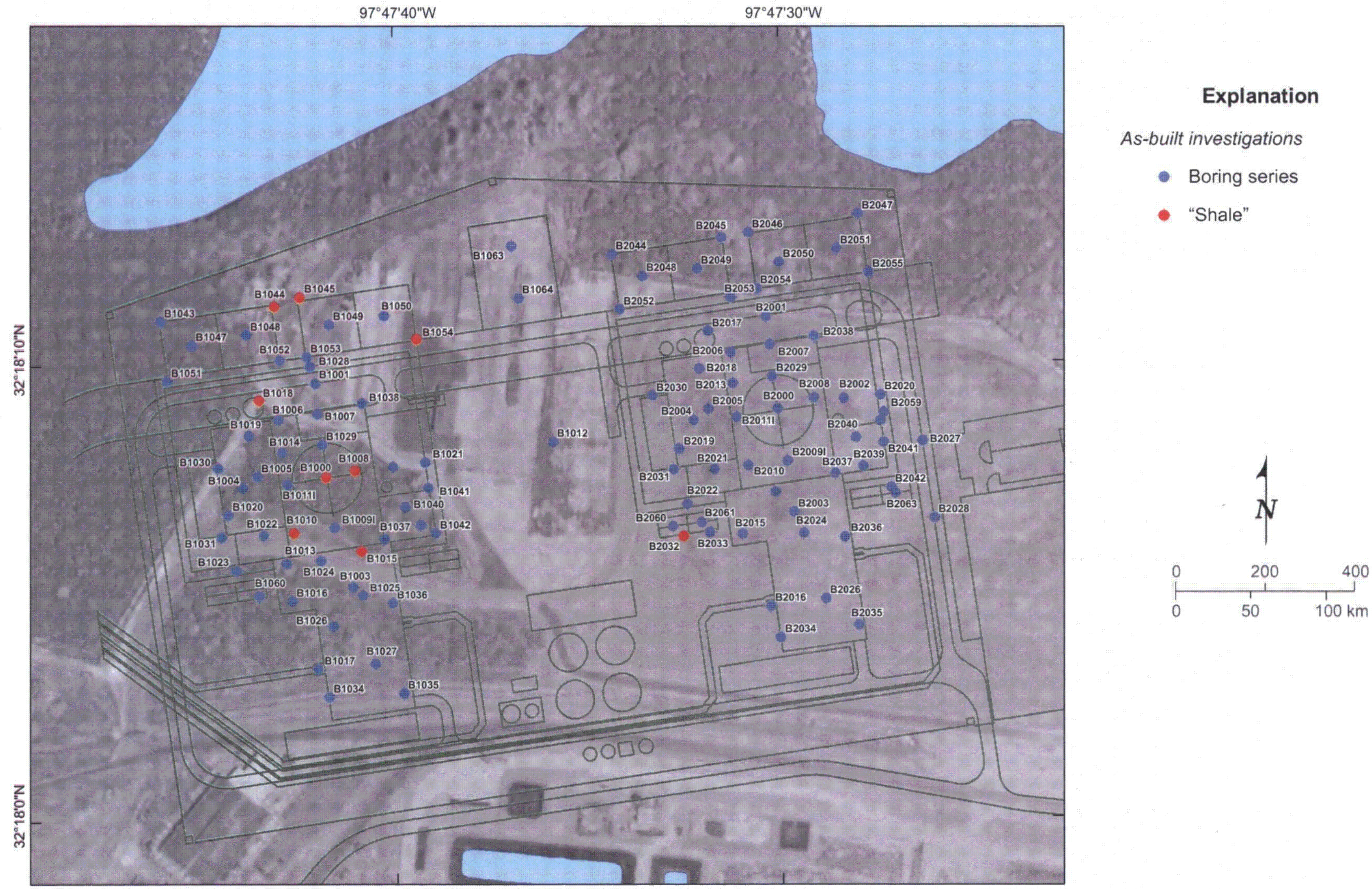

Sources: WGI "70607 FINAL site plan A.dwg"
Point Locations provided by GDM As-Built

Projection: NAD83 State Plane,
Texas North Central (ft)

Shale Beds within CS1 of Layer C
FIGURE 2.5.4-1-9

Rev 0

COMANCHE PEAK NUCLEAR POWER PLANT
UNITS 3 AND 4

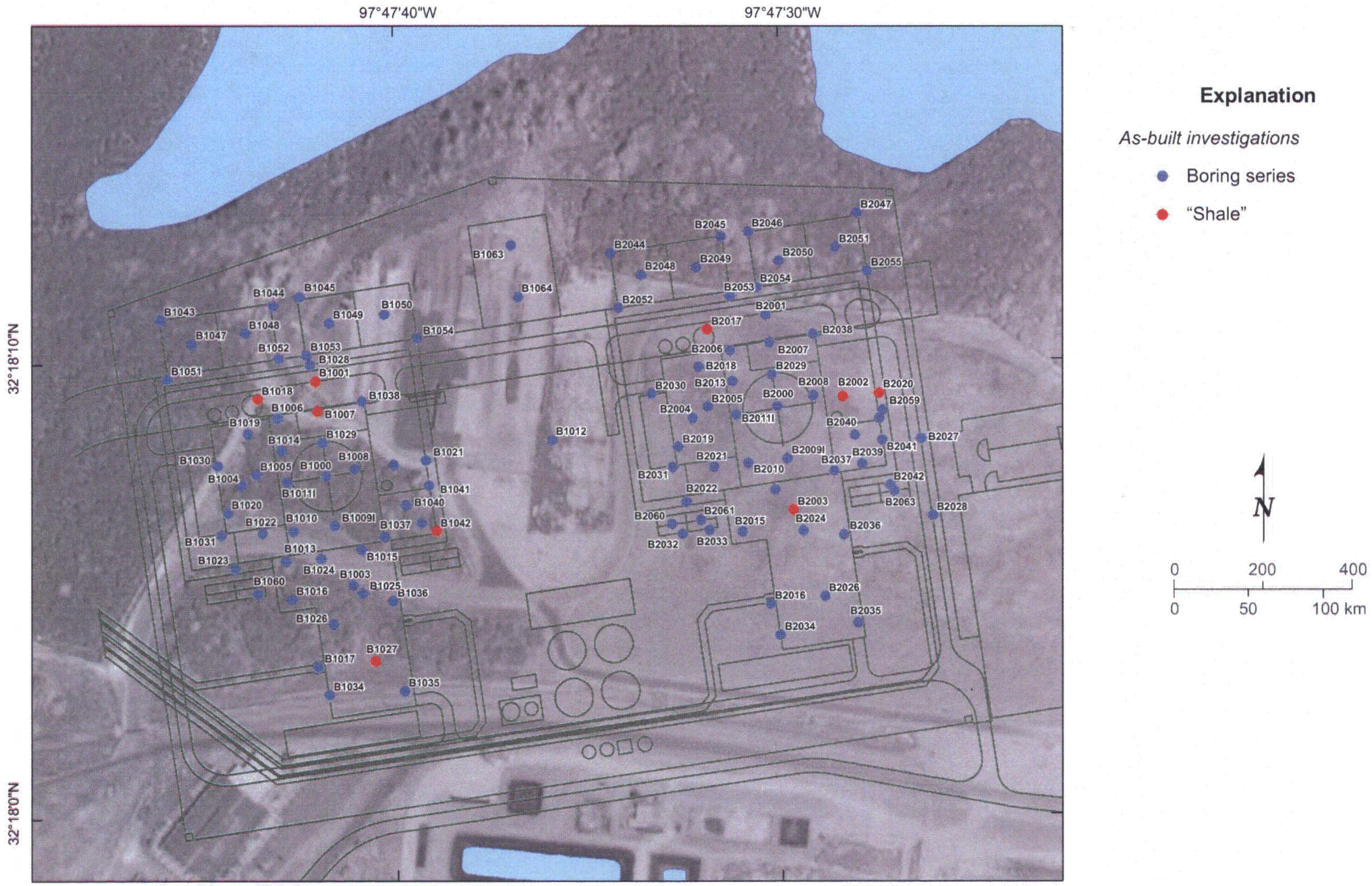

Sources: WGI "70607 FINAL site plan A.dwg"
Point Locations provided by GDM As-Built

Projection: NAD83 State Plane,
Texas North Central (ft)

Shale Beds within CS2 of Layer C
FIGURE 2.5.4-1-10

Rev 0

COMANCHE PEAK NUCLEAR POWER PLANT
UNITS 3 AND 4

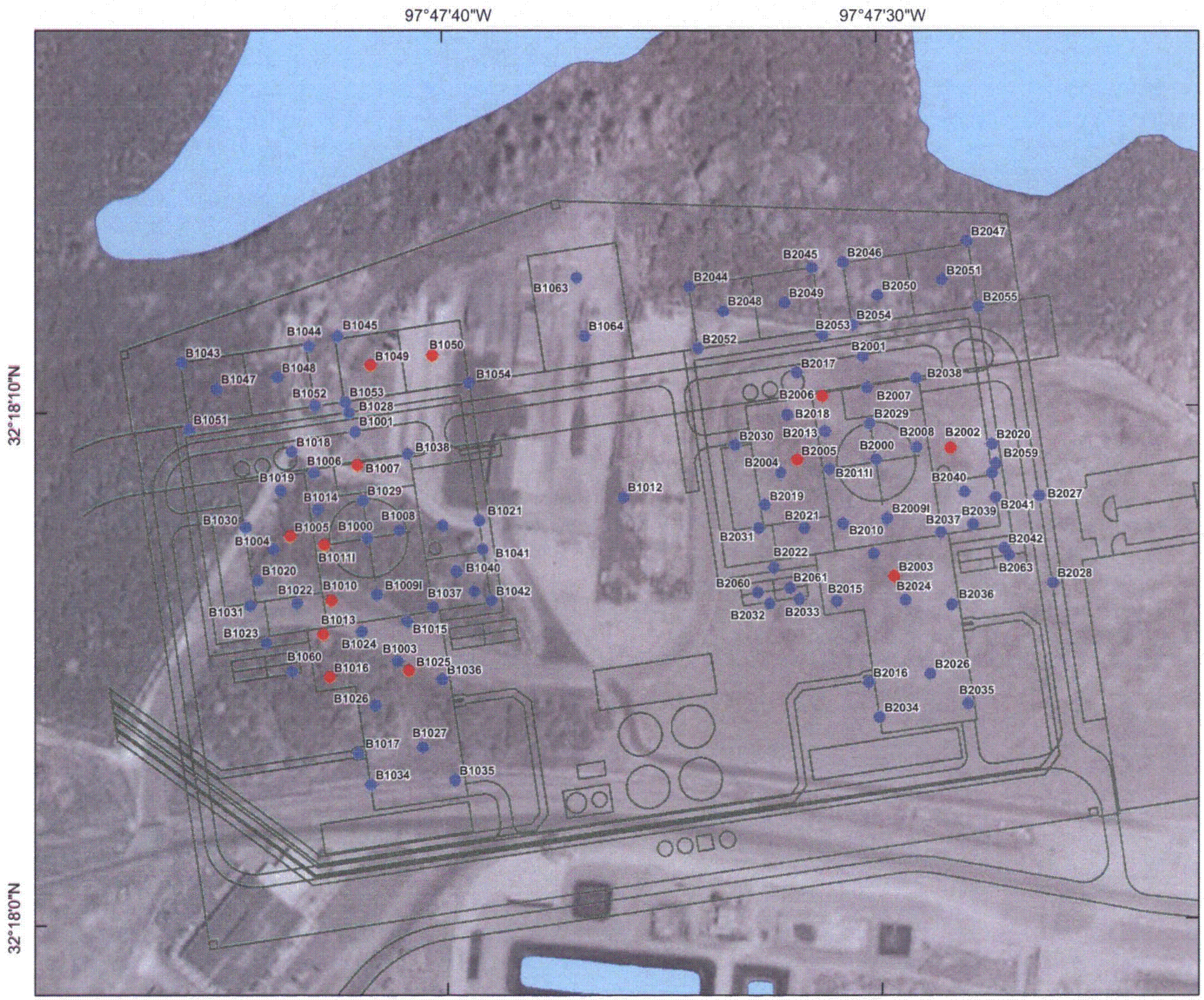

Explanation

As-built investigations

- Boring series
- "Shale"

N

0 200 400 ft

0 50 100 km

Sources: WGI "70607 FINAL site plan A.dwg"
Point Locations provided by GDM As-Built

Projection: NAD83 State Plane,
Texas North Central (ft)

Shale Beds within CS3 of Layer C
FIGURE 2.5.4-1-11

Rev 0

COMANCHE PEAK NUCLEAR POWER PLANT
UNITS 3 AND 4

COMANCHE PEAK NUCLEAR POWER PLANT
UNITS 3 AND 4

Shale Beds within CS4 of Layer C
FIGURE 2.5.4-1-12

Rev 0

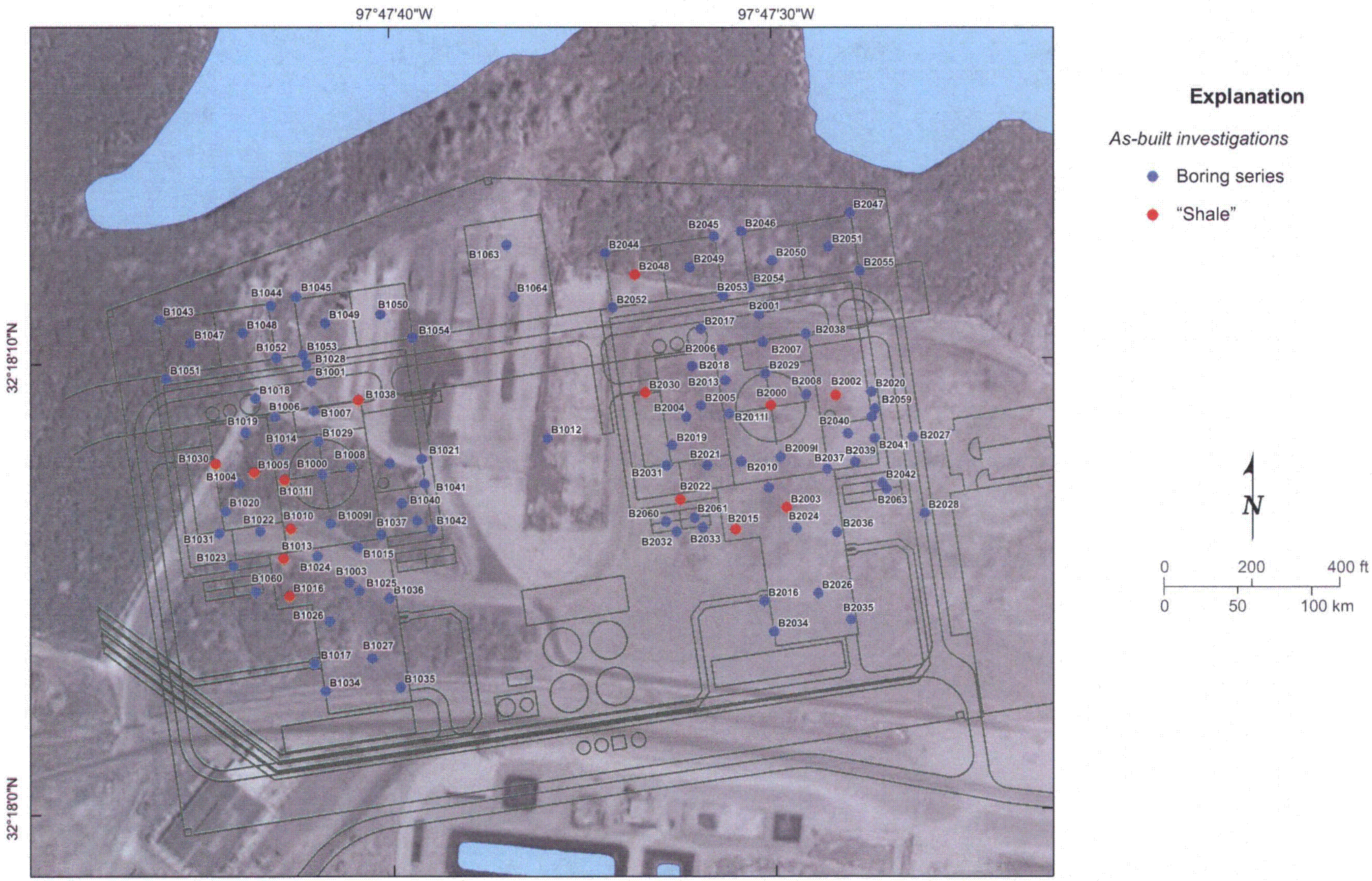

Sources: WGI "70607 FINAL site plan A.dwg"
Point Locations provided by GDM As-Built

Projection: NAD83 State Plane,
Texas North Central (ft)

RESPONSE TO REQUEST FOR ADDITIONAL INFORMATION

Comanche Peak, Units 3 and 4

Luminant Generation Company LLC

Docket Nos. 52-034 and 52-035

RAI NO.: 2929 (CP RAI #22)

SRP SECTION: 02.05.04 - Stability of Subsurface Materials and Foundations

QUESTIONS for Geosciences and Geotechnical Engineering Branch 1 (RGS1)

DATE OF RAI ISSUE: 7/17/2009

QUESTION NO.: 02.05.04-2

NUREG-0800, Standard Review Plan (SRP), Chapter 2.5.4, "Stability of Subsurface Materials and Foundations," establishes criteria that the NRC staff intends to use to evaluate whether an applicant meets the NRC's regulations.

Section 2.5.4.1.2 (page 124) of the FSAR indicates that the materials beneath the footprint of the facilities may contain localized zones or thin beds of poorly cemented or soft materials. These materials are discounted from having an important effect on response of performance or stability of the plant foundations on the basis of the small percentage of thickness of these materials as compared to the total thickness of the layer. Please provide information on the variability of these softer materials across the footprint of the facilities, and describe any potential impact these softer materials have on soil-structure interaction and structural response of the basemat. Please provide specific criteria on assessing their impact on uniformity assessments.

ANSWER:

Reference the response to Question 02.05.04-1 of RAI No. 2929 (CP RAI #22) for a discussion on subsurface uniformity.

The seismic Category I structures are to be founded directly on engineering Layer C which consists primarily of a 60-ft thick limestone with a mean shear wave velocity of about 5800 feet/sec. The uniformity of Layer C has been determined from the review of 114 core borings which penetrated the entire layer, primarily in the Reactor Building footprint and other seismic Category I and II structures. The vertical and lateral distribution of shale was quantified for each boring to assess both the total cumulative percentage of shale within Layer C as well as the lateral continuity of shale layers between borings. During the review of the core boring descriptions, four specific characteristics of intervals described as "shale" were noted, two of which are likely fine grained carbonate (micrite) as opposed to actual shale. However, for the purpose of this evaluation, each interval described as "shale" is included for conservatism.

From the compilation of boring log descriptions evaluated, the total percentage of shale within Layer C is approximately 1 percent of the total interval cored. As shown on Figures 2.5.4-1-5 and 2.5.4-1-6, the cumulative percentage of all shale layers for each boring are projected to a common latitude and longitudinal profile showing the CPNPP R/B approximate centerlines. With the exception of boring B-2002 which has a total of almost 11 cumulative feet of shale, the mean cumulative shale for all borings is less than 2 feet (1.2 percent) of Layer C.

The presence of laterally continuous shale layers was determined by plotting the thickness of shale within each boring at the respective elevation as shown on Figure 2.5.4-1-7 and 2.5.4-1-8. Four shale horizons (CS1, CS2, CS3 and CS4) were identified and plotted in plan view to determine the lateral extent, as shown on Figures 2.5.4-1-5 through 2.5.4-1-8. The interface between the overlying Layer B2 and Layer C beneath the Unit 4 indicates limited zones of shale in the range of elevation 782 which is the estimated mean average top elevation of Layer C. Subsection 2.5.4.12.8 provides a commitment that top of foundation inspections will identify shale pockets for removal prior to placement of fill or structural concrete.

The site response and soil structure interaction (SSI) analyses included the effect of thin beds of poorly cemented soil materials. The subgrade profiles used for the analyses include a 3-ft thick layer of a softer shale material within the Layer C limestone stratum. The shale layer is located at nominal elevation 717 ft or 65 ft below the bottom of the common mat foundation of the Reactor Building R/B complex consisting of the Prestressed Concrete Containment Vessel (PCCV), Reactor Building (R/B) and the containment internal structures. The table below presents the log mean or the best estimate of the dynamic properties of the thin shale layer considered in the site response and SSI analyses. The dynamic properties of the limestone layers located immediately above and below the thin shale layer are also presented in the table.

The methodologies used for the site response and SSI analyses are based on the assumption of infinite horizontal layering of the site and as such cannot explicitly account for spatial variability of the subgrade properties in the horizontal direction. Besides the best estimate values listed in the table, the SSI analyses used lower and upper bound soil properties to account for the uncertainties in the computed seismic response in accordance with SRP 3.7.2 Acceptance Criterion 4.

TOP ELEVATION (FT)	UNIT AND LITHOLOGY	UNIT WEIGHT (PCF)	POISSOIN'S RATIO	VS (FT/S)	VP (FT/S)	DAMPING (%)
782	LIMESTONE (FOUNDATION LAYER)	155	0.33	5685	11286	1.80
717	SHALE	135	0.42	3019	8129	2.00
714	LIMESTONE	155	0.36	4943	10569	1.80
690	LIMESTONE	155	0.31	6880	13111	1.80

Impact on R-COLA

None.

Impact on S-COLA

None.

Impact on DCD

None.

Attachments

Figures 2.5.4-1-5 – Latitudinal Profile Showing Shale Thickness in Layer C

Figures 2.5.4-1-6 – Longitudinal Profile Showing Shale Thickness in Layer C

Figures 2.5.4-1-7 – Areas with Shale Beds at Various Locations within Layer C below Unit 4

Figures 2.5.4-1-8 – Areas with Shale Beds at Various Locations within Layer C below Unit 3

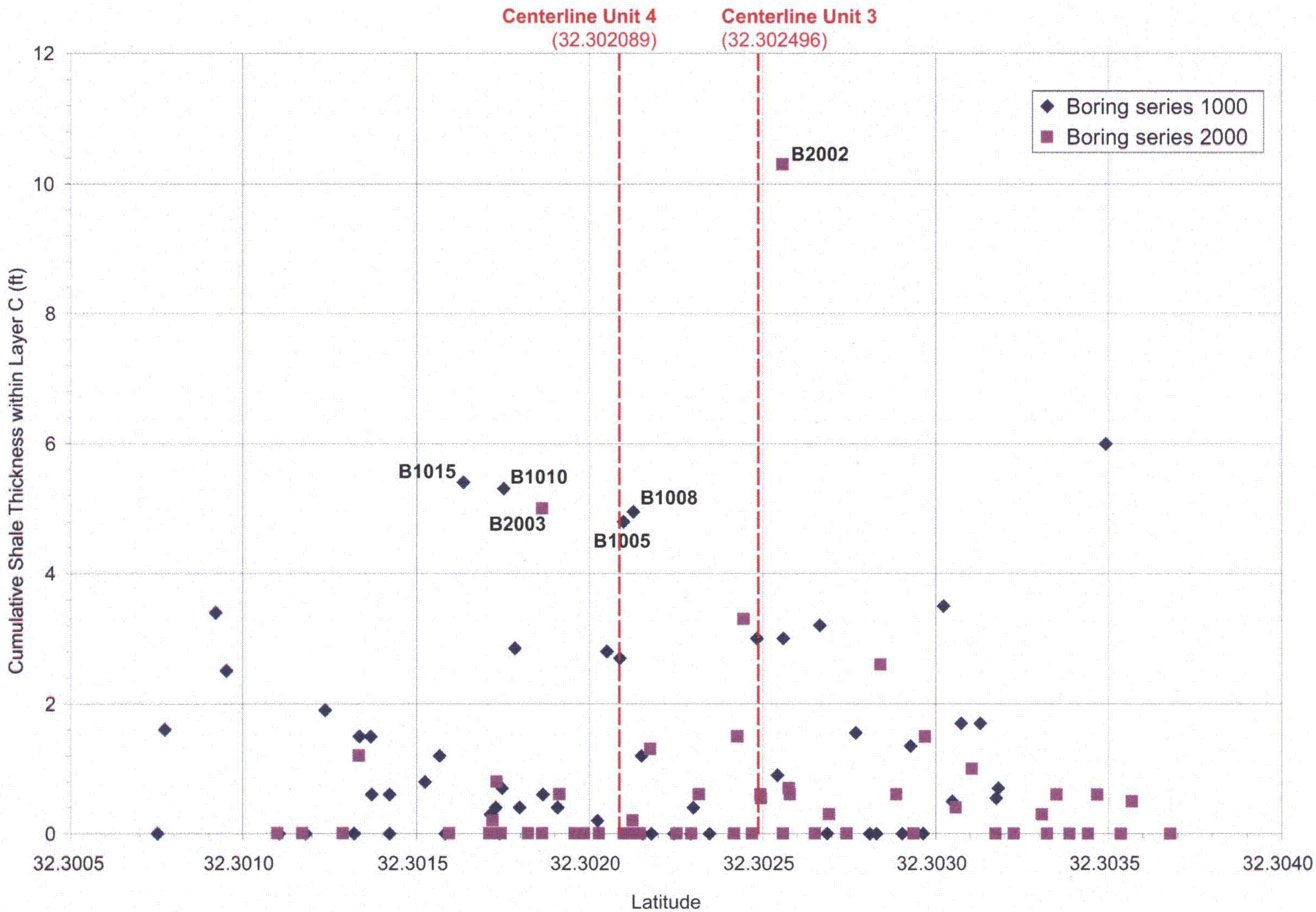

COMANCHE PEAK NUCLEAR POWER PLANT
UNITS 3 AND 4

Latitudinal Profile Showing Shale Thickness in Layer C
FIGURE 2.5.4-1-5
Rev 0

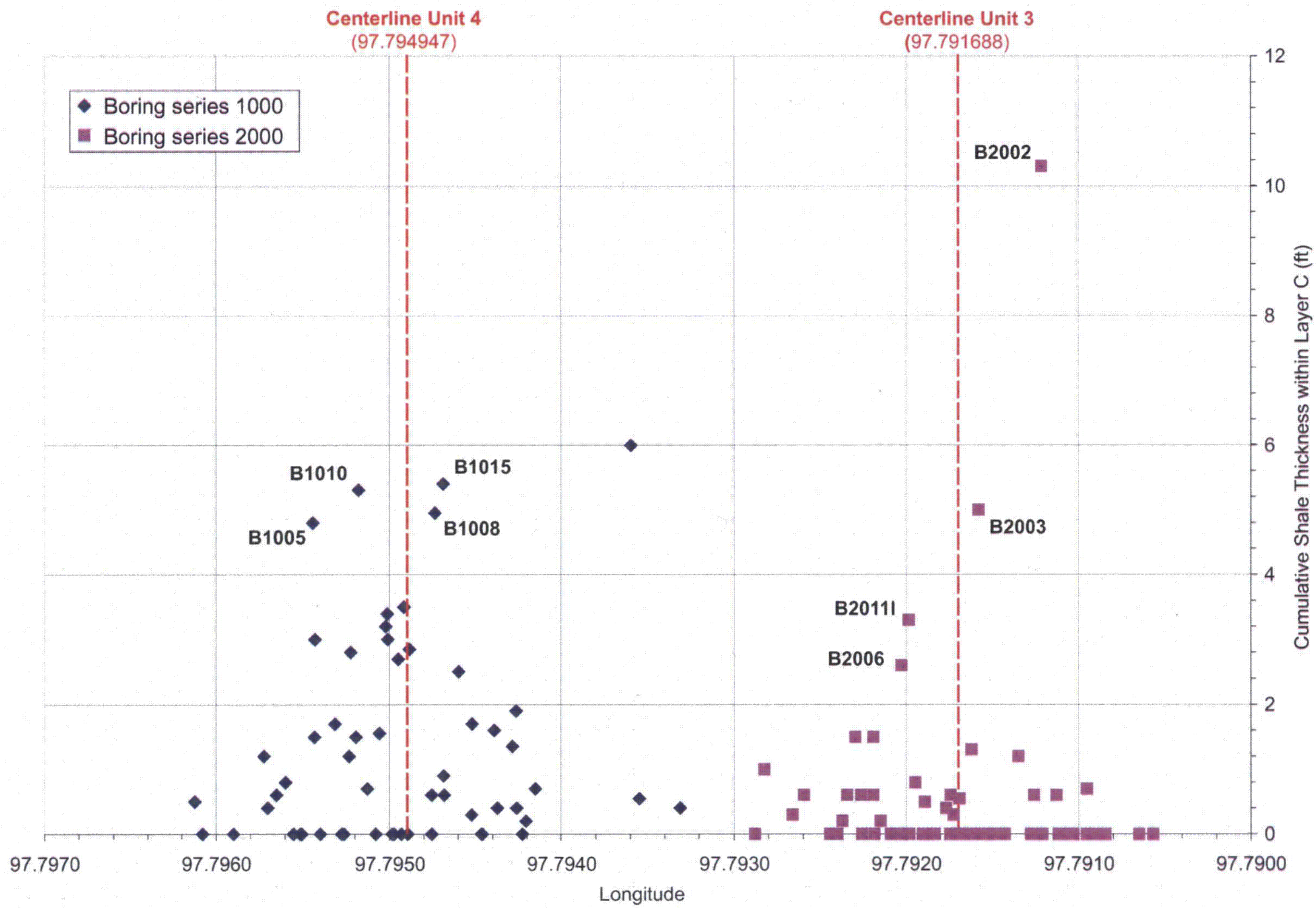

COMANCHE PEAK NUCLEAR POWER PLANT
UNITS 3 AND 4

Longitudinal Profile Showing Shale Thickness in Layer C
FIGURE 2.5.4-1-6
Rev 0

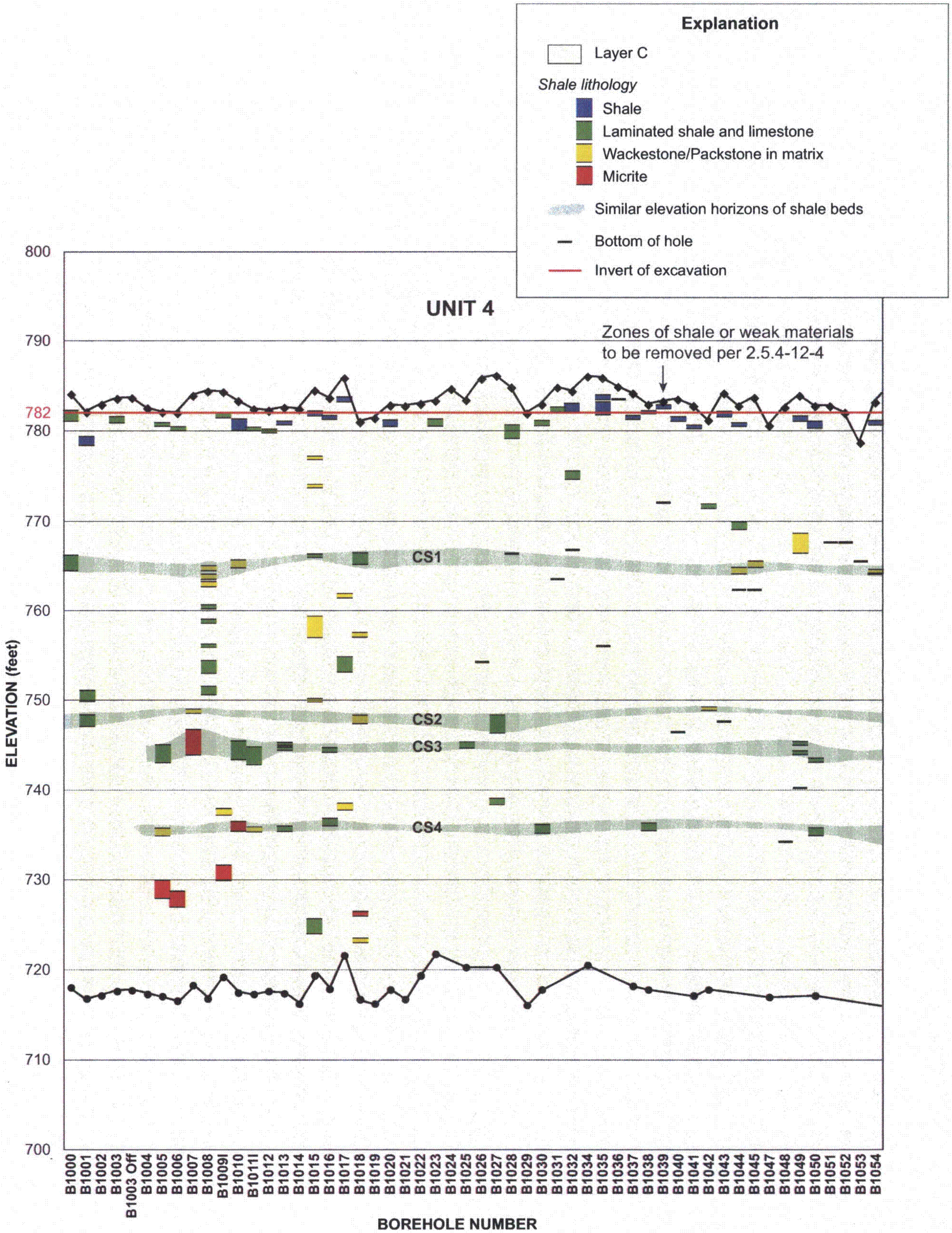

Areas with Shale Beds at Various Locations within Layer C below Unit 4

FIGURE 2.5.4-1-7 Rev 0

COMANCHE PEAK NUCLEAR POWER PLANT
UNITS 3 AND 4

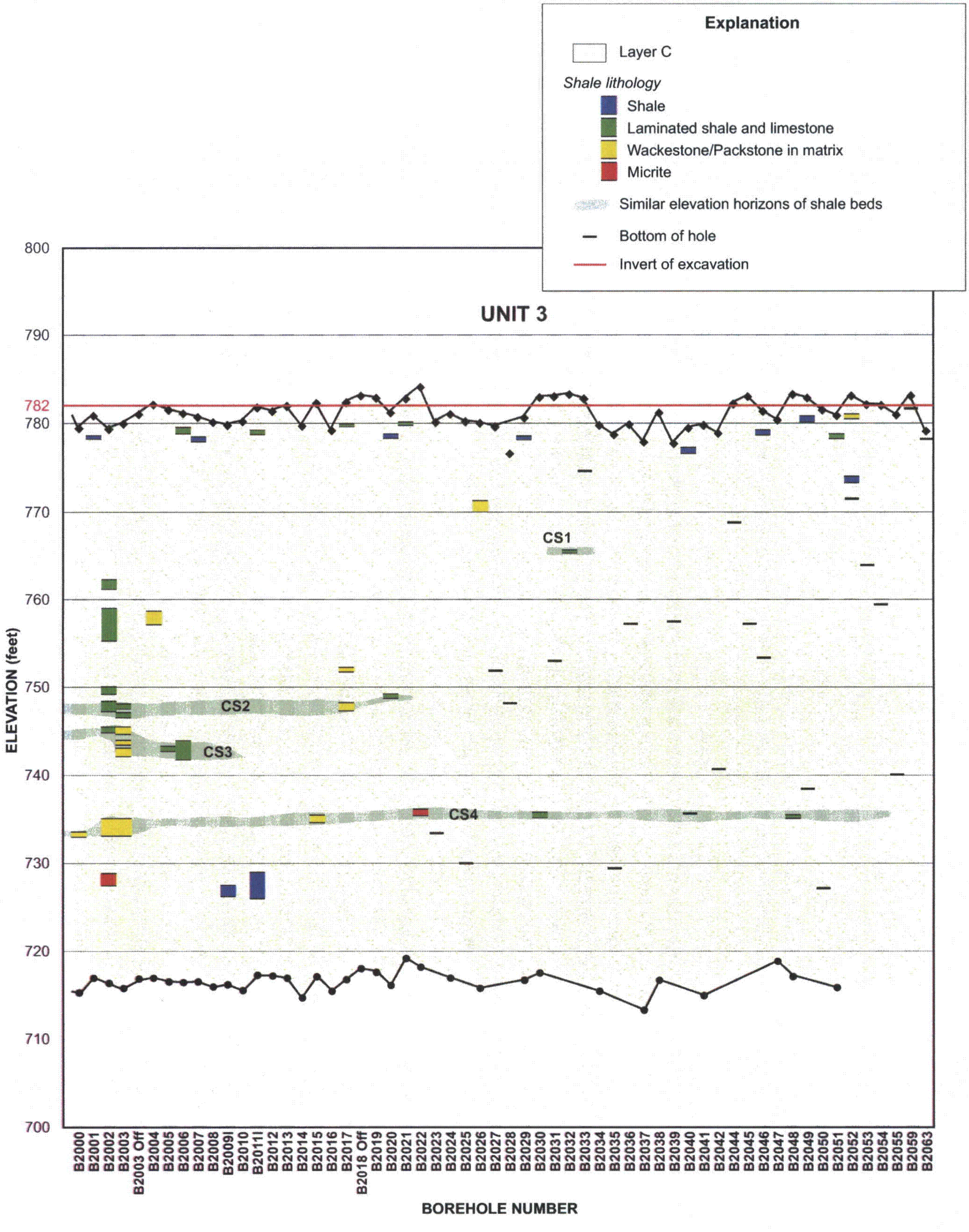

Areas with Shale Beds at Various Locations within Layer C below Unit 3

FIGURE 2.5.4-1-8 Rev 0

COMANCHE PEAK NUCLEAR POWER PLANT
UNITS 3 AND 4

RESPONSE TO REQUEST FOR ADDITIONAL INFORMATION

Comanche Peak, Units 3 and 4

Luminant Generation Company LLC

Docket Nos. 52-034 and 52-035

RAI NO.: 2929 (CP RAI #22)

SRP SECTION: 02.05.04 - Stability of Subsurface Materials and Foundations

QUESTIONS for Geosciences and Geotechnical Engineering Branch 1 (RGS1)

DATE OF RAI ISSUE: 7/17/2009

QUESTION NO.: 02.05.04-3

NUREG-0800, Standard Review Plan (SRP), Chapter 2.5.4, "Stability of Subsurface Materials and Foundations," establishes criteria that the NRC staff intends to use to evaluate whether an applicant meets the NRC's regulations.

Section 2.5.4.2.3.3 of the FSAR discusses the dynamic properties of rock and soil, but only discusses shear wave velocity and damping properties, and indicates that these were determined from the geophysical program. . Please provide additional information about how material damping was measured for both S- and P-wave velocities, and how material hysteretic damping was determined for site materials for both the shallow and deep velocity profiles.

ANSWER:

Shear (S) and compression (P) wave velocity measurements as well as rock lithology (limestone, shale and sandstone) and mass properties determined from the core data such as Rock Quality Designator (RQD), recovery and resistivity measurements indicate that the subsurface profile is stiff based on S and P wave velocities [see the response to Question 02.05.04-1 of RAI No. 2929 (CP RAI #22) for a discussion of uniformity and parameters used to assess mass properties]. Thus, the measured shear wave velocities were used to develop shear modulus (Gmax). The G/Gmax and damping variation with strain were developed for each rock lithology based on confinement depth in consultation with Dr. Ken Stokoe, Professor at University of Texas in Austin. This variation simulates typical non-linear hysteretic behavior of these materials as a function of strain. A discussion of these non-linear properties is provided in Appendix 2 of Project Report TXUT-001-PR-007, which was docketed as an attachment to Luminant letter TXNB-09049 on September 28, 2009 (ML092740182).

<u>Impact on R-COLA</u>

None.

Impact on S-COLA

None.

Impact on DCD

None.

RESPONSE TO REQUEST FOR ADDITIONAL INFORMATION

Comanche Peak, Units 3 and 4

Luminant Generation Company LLC

Docket Nos. 52-034 and 52-035

RAI NO.: 2929 (CP RAI #22)

SRP SECTION: 02.05.04 - Stability of Subsurface Materials and Foundations

QUESTIONS for Geosciences and Geotechnical Engineering Branch 1 (RGS1)

DATE OF RAI ISSUE: 7/17/2009

QUESTION NO.: 02.05.04-4

Calculation No. TXUT-001-FSAR-2.5-CALC-004 "Engineering Stratigraphy" indicates measured variability of the stratigraphic profile in the vicinity of the power block structures. Please provide additional information to demonstrate that this variability is within the range associated with the uniformity assumptions made in the site response and soil-structural interaction analyses conducted to estimate seismic response.

ANSWER:

The site response analyses use randomized soil profiles that are based on the stratigraphic profiles and consider appropriate variation of the shear wave velocities and compression wave velocities as presented in FSAR Table 2.5.2-227. The site specific ground motions that are developed based on the results of the site response analyses inherently account for the variability of the soil properties. The SSI analyses consider seismic input motion that is based on the minimum design earthquake requirements and envelopes by considerable margin the site-specific design input motion derived from the site response analyses. Therefore, it can be concluded with high level of confidence that that the design ground motion used in the SSI analysis adequately address the uncertainties due to the variability of the stratigraphic profile. Further, the responses to Questions 02.05.04-1 and 02.05.04-2 of RAI No. 2929 (CP RAI #22) have addressed potential variations in the stratigraphic profile engineering properties due to the presence of shale inclusions, and have concluded that those variations are insignificant and adequately covered by the ranges of engineering properties presented in Table 2.5.2-227.

The site-specific SSI analyses, including the seismic input motions used, are discussed in detail in Section 3.7 and Appendices 3KK, 3LL, 3MM, and 3NN. The SSI analyses consider seismic input motion that is based on and envelopes the input motion derived from the site response analyses, and therefore inherently considers the profile variations discussed above. The seismic input motion used for SSI analyses is explained further in the response to Questions 03.07.01-1, 03.07.01-2, 03.07.01-3, and 03.07.01-5 of RAI No. 2876 (CP RAI #55) in Luminant letter TXNB-09058 dated October 26, 2009.

Further, the SSI analyses consider input dynamic properties of the subgrade based on the stratigraphic profiles provided in Table 2.5.2-227 of the FSAR. The properties of the three profiles used in the SSI analyses representing lower bound (LB), best estimate (BE) and upper bound (UB) subgrade properties are used. The BE subgrade properties are consistent with the properties presented in FSAR Table 2.5.2-227. The analyses consider UB and LB estimates of the subgrade dynamic properties to ensure that potential variation of the stratigraphic profiles is adequately captured. A coefficient of variation (C_v) of 0.69 was used to develop the UB and LB properties of the subgrade.

Based on SRP 3.7.2, the LB and UB values of the soil dynamic shear modulus are calculated as:

$$G_{LB} = \frac{G_{BE}}{\left(1 + Cv^{(LB)}\right)} \qquad\qquad G_{UB} = G_{BE} \cdot \left(1 + Cv^{(UB)}\right)$$

The seismic evaluation and design is based on the envelope of the results obtained from the best estimate (BE), lower bound (LB), and upper bound (UB) SSI analyses consistent with the provisions of SRP 3.7.2 Acceptance Criterion 4.

<u>Impact on R-COLA</u>

None.

<u>Impact on S-COLA</u>

None.

<u>Impact on DCD</u>

None.

RESPONSE TO REQUEST FOR ADDITIONAL INFORMATION

Comanche Peak, Units 3 and 4

Luminant Generation Company LLC

Docket Nos. 52-034 and 52-035

RAI NO.: 2929 (CP RAI #22)

SRP SECTION: 02.05.04 - Stability of Subsurface Materials and Foundations

QUESTIONS for Geosciences and Geotechnical Engineering Branch 1 (RGS1)

DATE OF RAI ISSUE: 7/17/2009

QUESTION NO.: 02.05.04-9

NUREG-0800, Standard Review Plan (SRP), Chapter 2.5.4, "Stability of Subsurface Materials and Foundations," establishes criteria that the NRC staff intends to use to evaluate whether an applicant meets the NRC's regulations.

Sections 2.5.4.1.5 and 2.5.4.5.1 of the FSAR indicate that the power block structures are set back from the top of the reservoir slopes about 150' to 200', and that no evidence of previous landsliding has been found. Please clarify whether there are any assessments for the adequacy of this standoff distance to provide sufficient support for soil-structural interaction and lateral sliding. Also, please provide the specific evaluations performed to indicate that this standoff distance has been taken into account, and identify whether there have been any impacts to the stability evaluation for facilities of the plan area of the power blocks.

ANSWER:

Seismic analysis and design of structures is performed such that the stability of the structures is not dependent upon the standoff distance from the top of reservoir slopes cited above. This is explained further as follows.

Seismic Category I and II buildings at the site are founded directly on the Glen Rose Formation Layer C limestone, or a thin layer of fill concrete placed between the bottom of the building foundation and the limestone. The lateral sliding stability of structures does not rely on the stability of the reservoir slopes. As discussed in the response to Question 02.05.04-18 of RAI No. 2929 (CP RAI #22) provided in Luminant letter TXNB-09042 dated September 10, 2009 (ML092580684), resistance of structures to lateral loads is achieved by friction between the foundation basemat and by shear keys, where needed. Passive soil resistance is not relied upon to resist lateral loads. Further, friction resistance acting on the side walls of embedded structures is not relied upon to resist lateral loads. Shear keys transfer lateral loads by lateral bearing on the limestone and/or lateral bearing on fill concrete.

Site-specific soil-structure interaction (SSI) analyses are performed for structural design, as described in detail in Subsection 3.7 and Appendices 3KK, 3LL, 3MM, and 3NN. The SSI analyses consider a wide range of conditions in order to account for the effects of variability of the embedment and surface conditions. The following conditions are considered:

- No-fill (surface foundation) condition
- Foundation embedded in soil with Lower Bound (LB) properties
- Foundation embedded in soil with Best Estimate (BE) properties
- Foundation embedded in soil with Upper Bound (UB) properties
- Foundation embedded in soil with High Bound (HB) properties

Based on SRP 3.7.2, the LB, UB and HB values of the soil dynamic shear modulus are calculated as:

$$G_{LB} = \frac{G_{BE}}{\left(1 + Cv^{(LB)}\right)} \qquad G_{UB} = G_{BE} \cdot \left(1 + Cv^{(UB)}\right) \qquad G_{HB} = G_{BE} \cdot \left(1 + Cv^{(HB)}\right)$$

The best estimate (BE) values for soil shear modulii (GBE) are obtained from Table 2.5.2-227 of the CPNPP FSAR. A coefficient of variation (C_v) of 0.69 was used to develop the UB and LB properties of the subgrade and backfill. Additionally, the maximum variations of the embedment stiffness considered a C_v = 1.25 for the HB, and also considered the no-backfill condition. These variations envelop the variations of embedment stiffness specified in Table 2.5.2-227.

The SSI analyses used stiffness and damping properties of the embedment soil that are compatible with the strains generated by the input design SSE motion that is based on the minimum design earthquake requirement. The strain-compatible properties were obtained from a set of SHAKE 1-D wave propagation analyses that used as input the small strain LB, BE, UB and HB embedment soil properties and acceleration time histories compatible to the SSE design ground motion. The free field site response analyses considered the strain compatibility of the embedment soil by using degradation curves provided in FSAR Figure 2.5.2-232 that represent the stiffness and damping properties of the embedment soil as function of strain.

The analysis results of the conditions described above are enveloped for purposes of performing the structural designs. Because a "no-fill" (surface foundation only) condition is enveloped in the design, the structural design does not rely on the adequacy of the standoff distance to provide sufficient support for soil-structural interaction. Further, because the structural designs capture SSI embedment effects caused by the potential variations in the embedment conditions, the designs are not dependent on the standoff distance. Therefore, specific evaluations are not performed to take the standoff distance into account in the SSI analyses.

The stability of the reservoir slopes are evaluated and demonstrated in Subsection 2.5.5. The standoff distance has no impact to the stability evaluations for seismic category I and II facilities in the plan area of the power blocks because seismic category I and II building structures are founded on the Glen Rose Layer C limestone and the design does not rely on embedment or soil passive resistance for lateral support. The stability evaluations are based on seismic driving forces that envelop a wide variety of embedment effects including "no-fill" conditions.

<u>Impact on R-COLA</u>

None.

Impact on S-COLA

None.

Impact on DCD

None.

RESPONSE TO REQUEST FOR ADDITIONAL INFORMATION

Comanche Peak, Units 3 and 4

Luminant Generation Company LLC

Docket Nos. 52-034 and 52-035

RAI NO.: 2929 (CP RAI #22)

SRP SECTION: 02.05.04 - Stability of Subsurface Materials and Foundations

QUESTIONS for Geosciences and Geotechnical Engineering Branch 1 (RGS1)

DATE OF RAI ISSUE: 7/17/2009

QUESTION NO.: 02.05.04-10

NUREG-0800, Standard Review Plan (SRP), Chapter 2.5.4, "Stability of Subsurface Materials and Foundations," establishes criteria that the NRC staff intends to use to evaluate whether an applicant meets the NRC's regulations.

FSAR Figure 2.5.4-217 shows a general conceptual excavation cross-section. Please describe the procedure that will be followed during site excavation and construction activity to ensure that appropriate strata for proposed foundation locations, as described in the FSAR, are confirmed through objective measures and the exposed foundation laying surface is uniform. Any part of the contact surface of foundation that is shale and not Glen Rose limestone, should be removed and the remedial measures should be described in the FSAR. Please provide vertical and horizontal extent of all seismic categories I excavations, fills, and slopes, including the locations and limits of excavations, fills, and backfills on plot plans and geologic sections and profiles.

ANSWER:

FSAR Subsections 2.5.4.5.2, 2.5.4.5.4.3, 2.5.4.5.4.6.1, and 2.5.4.5.4.6.3 describe observations, geologic mapping, documentation, and monitoring during excavation. Continuous geologic mapping by qualified and trained geotechnical personnel and geologist is required during foundation excavation to verify that foundation quality materials are reached. Mapping is supplemented by additional objective measures including photographs, video tapes, and topographic survey of the excavation and pertinent geologic features. All excavation bottoms and foundation subgrades require observation, evaluation, and approval by qualified personnel prior to placing fill or concrete. These procedures confirm that uniform, suitable foundation materials are exposed at the base of foundation excavations.

In the event that unsuitable foundation materials are exposed at the base of excavations, FSAR Subsection 2.5.4.12.2 describes grouting and concrete dental repair below foundation subgrade elevations. Potential isolated zones of unsuitable material greater than 3 feet in maximum lateral dimension are excavated to sound rock and treated with fill concrete.

The allowable bearing capacity recommended for Glen Rose limestone (engineering Layer C) was determined using a compressive failure model, which ignores the contribution of embedment depth to capacity and confinement of the supporting strata. This model provides a very conservative estimate of bearing capacity for the current power block configuration, given that the foundations at the base of the Units 3 and 4 excavation will be embedded, on average, 40 feet below finished grade. While shale material exposed at the base of the excavation could be subject to undesirable desiccation, drying, and shrinkage, the presence of localized, relatively thin shale layers (as encountered in the borings) left unexposed below the surface of the excavation will not adversely impact the ultimate bearing capacity recommended for engineering Layer C. The measures described above will mitigate the impact of shale material exposed at the excavation surface on engineering Layer C bearing capacity.

Conceptual guidelines for the Units 3 and 4 excavation are shown on FSAR Figure 2.5.4-217 and described in FSAR Subsection 2.5.4.5.2. These guidelines provide the basic information for temporary excavation in both rock and fill soils around the seismic category I and II structures. The actual detailed excavation drawings will be developed based on these main excavation guidelines as part of the construction activities during the construction phase of the project. Detail beyond the conceptual excavation information that has already been provided such as lateral extend or aerial shape of the excavation, is not necessary for the purposes of site-specific soil-structure interaction (SSI) and lateral sliding analyses because side backfill is not relied upon for resistance. The response to Question 02.05.04-9 of RAI No. 2929 (CP RAI #22) explains that the site-specific SSI analyses consider a wide range of conditions to account for the effects of variability in embedment and surface conditions and backfill properties. The wide range of analyzed conditions will envelop the effects attributable to variations in the horizontal extent of excavation on the SSI analyses. Because a conservative set of assumptions was used for the analyses, details of the final excavation drawings beyond those shown in the conceptual excavation guidelines (FSAR Figure 2.5.4-217) will not affect the final outcome of the seismic and stability analyses of the seismic category I and II structures. However, detailed drawings addressing the vertical and horizontal extent of seismic category I excavations, fills, and slopes, including the locations and limits of excavations, fills, and backfills will be prepared at a later date during the construction phase of the project. These documents will be available for NRC review or audit once they have been completed.

Impact on R-COLA

None.

Impact on S-COLA

None.

Impact on DCD

None.

RESPONSE TO REQUEST FOR ADDITIONAL INFORMATION

Comanche Peak, Units 3 and 4

Luminant Generation Company LLC

Docket Nos. 52-034 and 52-035

RAI NO.: 2929 (CP RAI #22)

SRP SECTION: 02.05.04 - Stability of Subsurface Materials and Foundations

QUESTIONS for Geosciences and Geotechnical Engineering Branch 1 (RGS1)

DATE OF RAI ISSUE: 7/17/2009

QUESTION NO.: 02.05.04-17

NUREG-0800, Standard Review Plan (SRP), Chapter 2.5.4, "Stability of Subsurface Materials and Foundations," establishes criteria that the NRC staff intends to use to evaluate whether an applicant meets the NRC's regulations.

Section 2.5.4.10.1 of the FSAR indicates values of ultimate bearing capacity. Calculation No. TXUT-001-FSAR-2.5-CALC-009, "Settlement and Bearing Capacity," indicates that these were determined from standard formulae associated with static load conditions. The statement is made (FSAR page 189) that the ultimate bearing capacity of the Glen Rose Formation is 146 ksf. Please provide information on how dynamic effects were included in the assessment of ultimate bearing capacity, compare the ultimate bearing capacity with dynamic bearing demand, and assess safety factors under dynamic loads.

ANSWER:

As described in Subsection 2.5.4.10.1, three potential failure mechanisms (general shear failure, local shear failure, and compressive failure) are used for estimating the ultimate bearing capacity of the Glen Rose Formation engineering Layer C. The rock mass properties for bearing capacity evaluation were conservatively selected based on the lower bound results of the unconfined compression tests. Thirty-eight limestone samples and one limestone sample with shale interbeds from engineering Layer C were tested for unconfined compression. The unconfined compression strength values from the tests ranged between 73 and 812 tsf (146 to 1624 ksf) for the limestone samples and 91 tsf (182 ksf) for the limestone sample with shale interbeds (see FSAR Figure 2.5.4-226). The angle of internal friction is conservatively assumed to be zero and the cohesion is assumed to be 73 tsf for the bearing capacity calculation of the engineering Layer C materials. The compressive failure mode results in a static ultimate bearing capacity of 146 ksf. This mode of failure occurs when a foundation is supported on a poorly constrained (laterally) column of rock, and it is considered to be a very conservative model for the conditions at the CPNPP Units 3 and 4 site.

Based on dynamic tests performed by Professor Kenneth Stokoe (University of Texas at Austin) on similar rock materials, there are no indications that appreciable cyclic degradation would occur and result in a decrease in the bearing capacity of rock for the anticipated dynamic loads during the design seismic event. In addition, the dynamic shear modulus and shear strength (and hence the bearing capacity) of the type of rock encountered below the planned foundation elevation at the site are expected to be greater than the static values during fast dynamic loading conditions (i.e. strain rate effects). Potential damage to the rock structure and strength as a result of dynamic loading is normally associated with large stress/strain, which is not a concern at this site with low seismic demand.

Considering the above discussion and the fact that the governing bearing capacity value (FSAR Table 2.5.4-228) is based on the very conservative compressive failure mode and the absolute minimum laboratory test data, the estimated static ultimate bearing capacity of 146 ksf is considered valid and conservative (lower bound value) for dynamic bearing capacity.

A comparison of the ultimate bearing capacity and the static and dynamic demands for seismic category I and II structures is provided in FSAR Table 3.8-202. The table shows that the ultimate bearing capacity compares very favorably to both the static and the dynamic bearing pressures, and provides an adequate margin of safety.

The total settlement analyses in Calculation TXUT-001-FSAR-2.5-CALC-009 (attached) included the following assumptions: 1) uniform distribution of foundation loads (including dead plus live loads) and 2) flexible foundation (i.e. contribution of the rigidity of the mat foundation in reducing the foundation settlement was conservatively ignored). Two independent deformation modulus models (Lower Bound and Best Estimate models) were developed to encompass the potential variability of rock mass properties across the site. The magnitude of total settlement for the center points of the main structures for the Lower Bound model was conservatively estimated and reported at about 0.37 inch.

Additional analyses were performed to consider the effects of: 1) non-uniform structural load distribution and 2) non-uniform support conditions (i.e. shear modulus of Glenn Rose Formation varying from the lower bound to the best estimate).

The Reactor Building (R/B) Complex foundation area was divided into seven zones based on preliminary estimates of the project-specific distribution of structural loads. Figure 1 shows an idealized approximation of the bearing pressures for each zone. Foundation settlements were calculated along seven north-south lines for both the lower bound and the best estimate/upper bound rock profiles.

The elastic modulus of foundation rock varied between the red profile and green profile shown on FSAR Figure 2.5.4-241. These values correspond to the lower bound and best estimate/upper bound limits, respectively. The calculated settlement corresponding to the lower bound and the best estimate/upper bound material properties are presented on attached Figures 2 and 3, respectively.

Settlement values calculated using the lower bound properties (Figure 2) are:

- The maximum foundation settlement is about 0.35 inch.
- The maximum differential settlement within or between any of the seven lines is less than 0.17 inch.
- Settlement values calculated using the best estimate/upper bound properties (Figure 3) are:
- The maximum foundation settlement is about 0.18 inch.
- The minimum foundation settlement is about 0.1 inch.

- The maximum differential settlement within or between any of the seven lines is less than 0.08 inch.

Using the information presented above, it is concluded that if the structure is supported partially on rock with the lower bound shear modulus profile, and partially on rock with the best estimate/upper bound shear modulus profile, the maximum differential settlement across the foundation along the seven lines shown on Figure 1 is about 0.25 inch [maximum 0.35 inch (Figure 2) - minimum 0.1 inch (Figure 3) = 0.25 inch]. Furthermore, this estimate is conservative because the rigidity of the mat was ignored in the settlement calculations.

<u>Impact on R-COLA</u>

None

<u>Impact on S-COLA</u>

None

<u>Impact on DCD</u>

None

<u>Attachments</u>

Figure 1 – R/B Load Areas for Settlement Calculation

Figure 2 – R/B Complex Settlement Estimates (LB Model)

Figure 3 – R/B Complex Settlement Estimates (BE Model)

TXUT-001-FSAR-2 5-CALC-009 Rev.1 - Settlement and Bearing Capacity (Attachment 4 to this letter)

RB Load Areas for Settlement Calculation

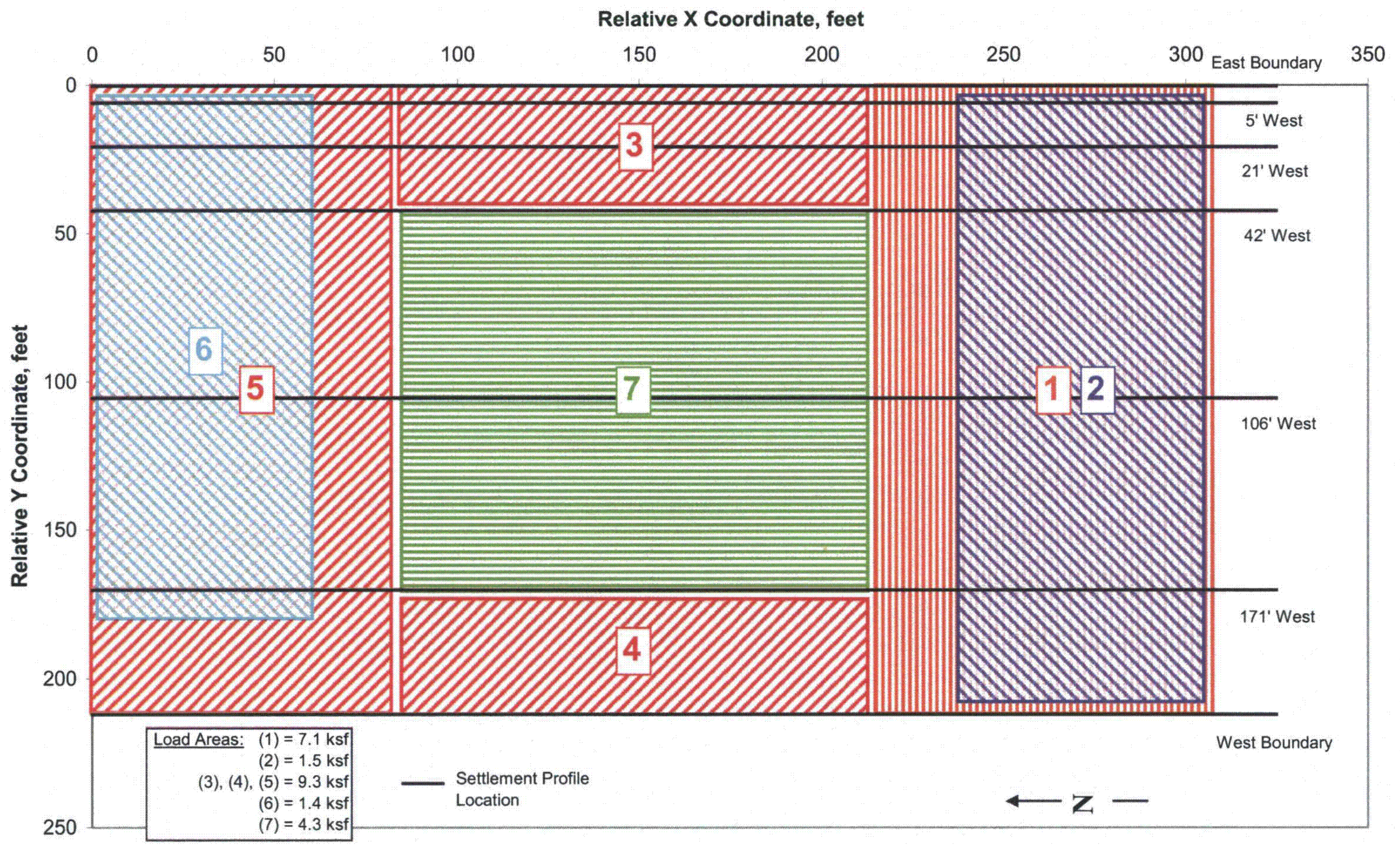

RAI 02.05.04-17
FIGURE 1

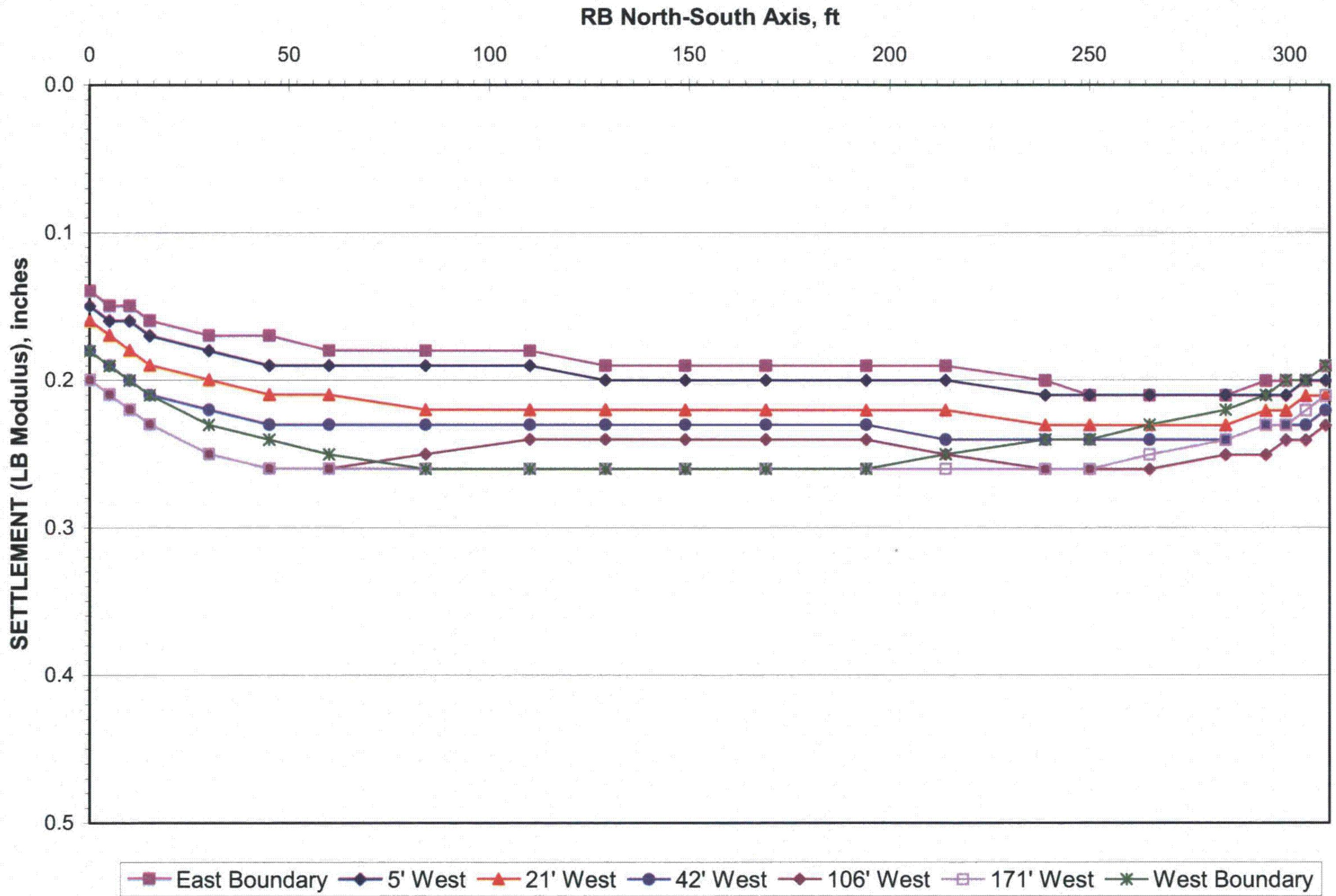

RAI 02.05.04-17
FIGURE 2

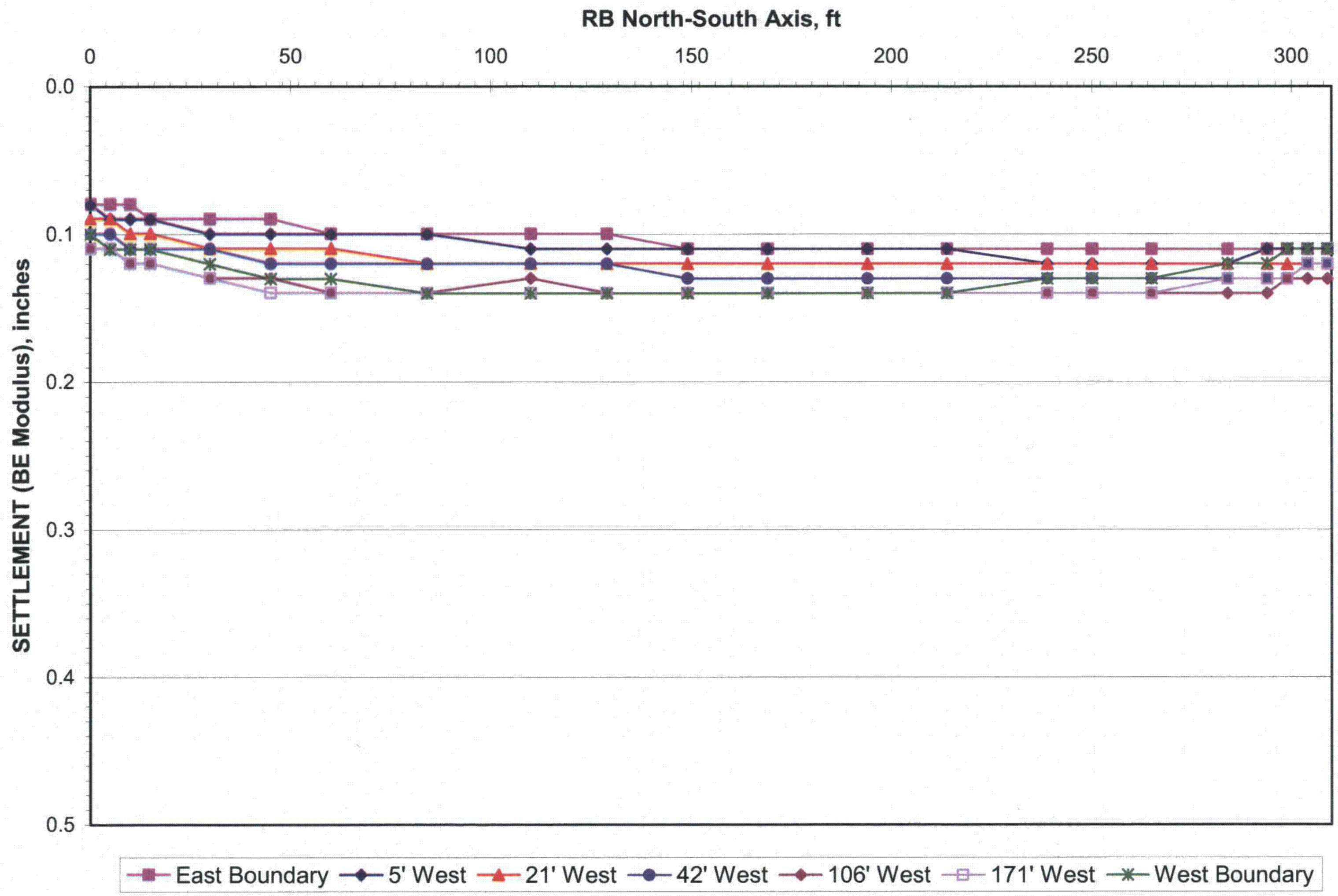

RAI 02.05.04-17
FIGURE 3

Attachment 3

Response to Request for Additional Information No. 2930 (CP RAI #19)

RESPONSE TO REQUEST FOR ADDITIONAL INFORMATION

Comanche Peak, Units 3 and 4

Luminant Generation Company LLC

Docket Nos. 52-034 and 52-035

RAI NO.: 2930 (CP RAI #19)

SRP SECTION: 02.05.05 - Stability of Slopes

QUESTIONS for Geosciences and Geotechnical Engineering Branch 1 (RGS1)

DATE OF RAI ISSUE: 7/14/2009

QUESTION NO.: 02.05.05-1

NUREG-0800, Standard Review Plan (SRP), Chapter 2.5.5, 'Stability of Slopes,' establishes criteria that the NRC staff intends to use to evaluate whether an applicant meets the NRC's regulations.

FSAR Section 2.5.5.2.5. states that a pseudo-static method was used for the slope stability analysis at the site. The guidance described in SRP 2.5.5.2 specifies that both vertical and horizontal motions be considered in the evaluation of slope stability. Demonstrate how the vertical motion was considered in the slope stability analyses.

ANSWER:

Initially, because the seismicity at the CPNPP Units 3 and 4 site is very low, only horizontal peak ground acceleration (PGA) was used with the yield acceleration approach to evaluate dynamic stability. However, the pseudo-static slope stability analyses have been updated to consider both horizontal and vertical ground motions.

Horizontal and vertical ground motions were considered in the analyses through the application of seismic coefficients to the potential slide mass. The magnitude of the horizontal coefficient was assumed to be equal to the US-APWR DCD minimum PGA of 0.10g. The magnitude of the vertical coefficient was conservatively set at 0.10g using a vertical to horizontal ratio equal to 1.0. This assumption is deemed to be conservative considering the regional-specific geologic and seismic setting including the magnitude and site-to-source distance of the controlling seismic sources.

Both positive (downward) and negative (upward) vertical coefficients were considered. For each individual cross section, the orientation resulting in the lower factor of safety was considered to be the critical condition.

Seismic slope performance is considered acceptable if pseudo-static slope stability analyses in which the horizontal and vertical seismic coefficients are assumed to be equal to the PGA result in factors of safety greater than 1.1. FSAR Table 2.5.5-203 has been revised to show the computed factors of safety range between 1.47 and 1.96. Those results demonstrate that the seismic performance of the analyzed slopes is acceptable and that no seismically induced permanent slope displacement is expected at CPNPP Units 3 and 4 sites during and after the design seismic event.

Impact on R-COLA

See attached marked-up FSAR Draft Revision 1 pages 2-liv, 2.5-217, 2.5-218, 2.5-219, 2.5-220, 2.5-243, Table 2.5.5-203, and Figures 2.5.5-213 through 2.5.5-216.

Impact on S-COLA

None.

Impact on DCD

None.

ACRONYMS AND ABBREVIATIONS

°F	degrees Fahrenheit
ΔT	vertical temperature difference
χ/Q	relative concentration, in sec/m^3
AADT	annual average daily traffic
ACFT	acre feet
ac-ft	acre feet
AF	amplification factor
AFB	Air Force Base
ALOHA	Areal Locations of Hazardous Atmospheres
AMRT	Average Mean Residence Time
ANL	Argonne National Laboratory
ANSS	Advanced National Seismic System
ASCE	American Society of Civil Engineers
ASHRAE	American Society of Heating, Refrigerating and Air-Conditioning Engineers RCOL2_02.03.01-1
~~a_y~~	~~yield acceleration~~ RCOL2_02.05.05-1
BB	Broad-Banded
BE	Best Estimate
bgs	below ground surface
BIS	Banks Information Solutions Inc.
BRA	Brazos River Authority
BRM	Brazos River Mile
BTS	Bureau of Transportation Statistics
CAV	Cumulative Absolute Velocity
C_d	overtopping discharge coefficient

2.5.5.2.3 Groundwater

Groundwater within the existing fill is controlled by the water level in the adjacent SCR. According to the USGS, the pool elevation of the SCR is normally about elevation 775 ft, and has historically fluctuated between elevations 773 ft and 778 ft. Filled swale areas northeast of CPNPP Unit 4 and east of Unit 3 extend to the reservoir shoreline. The fill appears to be in hydraulic communication with the reservoir, and a perched groundwater table at, or near, the elevation of the reservoir pool exists in the fill. According to the preliminary results from monitoring of field piezometers within the Units 3 and 4 area, the piezometric levels range between about elevation 775 ft and 858 ft, although some wells remain dry. Observed piezometric levels are considered to be localized perched water in the upper zone of the Glen Rose Formation and could possibly be attributed to surface run-off rather than a true indication of permanent groundwater at the site. Groundwater and hydrogeologic conditions of the site are discussed in detail in Subsection 2.4.12.

For the purposes of modeling the slope stability, the groundwater table was conservatively assumed to be at elevation 780 ft.

2.5.5.2.4 Slope Stability Analysis Methodology

The slope stability analyses were performed for static and dynamic (pseudo-static) loading conditions. The latter analysis was performed~~ in terms of yield accelerations calculations. Yield acceleration values are often used to estimate the permanent slope displacements~~using both horizontal and vertical seismic coefficients. RCOL2_02.05.05-1

Conventional two-dimensional limit-equilibrium analyses were performed considering permanent (long-term) slope stability conditions.

Various methods of analysis, including Janbu and Bishop's (References 2.5-428, 2.5-429, and 2.5-430), were used for initial screening of possible failure surface geometries. Various failure surface shapes were considered, including Rankine-type, random block, and circular surfaces. Refined analyses were performed using Spencer's method (Reference 2.5-431) on targeted failure surfaces identified by the screening analysis. Spencer's method is considered more appropriate as it satisfies both force and moment equilibrium.

Soil and rock materials that exhibit anisotropic shear strength properties are more appropriate to be modeled by assigning Mohr-Coulomb strength parameters with two sets of shear strength parameters: "along" and "across" bedding. For conservatism, only along-bedding shear strength parameters of the shale were used in the stability analysis of permanent slopes (Subsection 2.5.5.2.2.5). This approach was used to model the Glen Rose Formation shale beds. Hoek-Brown criteria for rock-mass shear strength parameters were used to model the massive Glen Rose Formation limestone.

The computer program Slope/W 2007 (Geo-Slope International) was used to perform the slope stability analyses. This program models heterogeneous soil types, soil and rock anisotropy, complex stratigraphic and slip surface geometry, and variable pore water pressure conditions. The program was validated and verified for these analyses.

2.5.5.2.5 Dynamic Slope Stability

A pseudo-static method of analysis was ~~adopted~~used for stability evaluation of the slopes at the project site. In this method, the effects of seismic loading conditions on the slopes are accounted for ~~by applying a constant horizontal seismic coefficient to the slope and computing a pseudo-static factor of safety. The seismic coefficient is increased and the stability analysis is repeated until the computed pseudo-static factor of safety approaches unity (i.e. the onset of instability and slope deformation). The seismic coefficient that would reduce the factor of safety from its static value down to unity is called the yield coefficient,~~ ~~k_y,~~ ~~and the corresponding pseudo-static acceleration is called yield acceleration,~~ ~~a_y~~ ~~($a_y = k_y g$).~~ through the application of constant horizontal and vertical seismic coefficients to the slope and computation of a pseudo-static factor of safety. With the conservative assumption of vertical-to-horizontal ration of 1.0 the magnitude of the vertical coefficient is taken equal to the horizontal PGA. Both positive (downward) and negative (upward) vertical coefficients were considered. The orientation resulting in the lower factor of safety is considered the critical condition. If pseudo-static slope stability analyses, in which the horizontal and vertical seismic coefficients are taken equal to the PGA, result in factors of safety greater than 1.1, seismic slope performance is considered acceptable. RCOL2_02.05.05-1 RCOL2_02.05.05-1

~~If the yield acceleration is higher than the peak ground acceleration (PGA) at the center of a potentially sliding mass, the slope is considered to be stable. If, however, the average PGA at the center of a potentially sliding mass is higher than the yield acceleration, the slope becomes unstable and experiences permanent deformation. The magnitude of deformation is dependent on the ratio of~~ ~~a_y~~ ~~to PGA and the earthquake magnitude. In this case, an order of magnitude of seismically induced permanent slope displacements can be estimated using a simplified procedure, such as the procedure proposed by Bray and Travasarou (Reference 2.5-427) or Makdisi and Seed (Reference 2.5-425).~~

Ground motion and site response analyses discussed in Subsection 2.5.2 indicate that the horizontal PGA corresponding to the GMRS and FIRS1 at the CPNPP Units 3 and 4 site is about 0.045g. Horizontal PGA corresponding to the other FIRS are all below 0.07g, as shown on Figures 2.5.2-234 and 2.5.2-239. RCOL2_02.05.05-1
Therefore, the US-APWR DCD minimum PGA of 0.10g is used as the design PGA for ~~comparison against the calculated~~ ~~a_y~~ ~~that was derived from~~both the horizontal and vertical seismic coefficients used in the slope stability modeling. RCOL2_02.05.05-1

2.5.5.2.6 Analyses

Each subsection was analyzed for the following conditions using Spencer's method. Permanent slopes at the site were considered, and analyses were performed for the cases of circular (rotational), block/wedge (translational), or random potential failure modes as follows:

- Global (deep-seated) stability conditions
- Surficial stability conditions
- Pseudo-static (seismic or transient) loading conditions

Surficial stability of the 2(H):1(V) compacted fill slopes was also analyzed using the procedure developed by the U.S. Army Corps of Engineers (Reference 2.5-426) for both the static and pseudo-static loading conditions.

External loading conditions modeled in the slope stability analyses consisted of structural loads, traffic loads, and earthquake loads. Traffic and construction loads were modeled on top of the fill slopes, assuming a uniform surcharge pressure of 250 psf.

The following minimum factors of safety were established for this analyses based on the U.S. Army Corps of Engineers' Slope Stability Manual (Reference 2.5-426):

- Static Long-Term Factor of Safety: 1.5
- Static Temporary Factor of Safety: 1.3
- Pseudo-static Factor of Safety: 1.1 RCOL2_02.05.05-1

2.5.5.2.7 Results

The results of slope stability analyses of the permanent slopes indicate acceptable static long-term and pseudo-static factors of safety with values greater than 1.5 and 1.1, respectively, as summarized in Table 2.5.5-203. ~~Examples of slope stability sections showing final critical circles, static factor of safety, and K_y-values are included as follows:~~ Example slope stability sections showing final critical circles and factors of safety are included as follows: RCOL2_02.05.05-1

- Figures 2.5.5-209, 2.5.5-210, 2.5.5-211, and 2.5.5-212 for static global stability of permanent slopes, including Cross Sections D-D', E-E', E1-E1', and F-F' through Units 3 and 4, and the area between them, respectively.
- Figures 2.5.5-213, 2.5.5-214, 2.5.5-215, and 2.5.5-216 for seismic global stability of permanent slopes, including Cross Sections D-D', E-E', E1-E1', and F-F', respectively.

The results of the surficial stability for 2(H):1(V) compacted fill slopes also indicate that the engineered compacted fill slopes do have adequate surficial slope stability factors of safety, provided that the compacted fill materials exhibit the specified effective cohesion value of at least 200 psf, and an effective friction angle of at least 32 degrees, in accordance with the engineered fill specification.

Factors of safety are summarized in Table 2.5.5-203. The estimated factors of safety for permanent slopes satisfy the minimum required value.

~~Estimated yield acceleration (a_y) values shown in Table 2.5.5-203 range between 0.31g to 0.44g. These yield acceleration values are all considerably greater than the comparative PGA of 0.1g, and exhibit high factors of safety for calculated GMRS and FIRS PGA values.~~Pseudo-static factors of safety were estimated using horizontal and vertical acceleration coefficients equal to 0.1g. The resulting factors of safety range between 1.47 and 1.96 (Table 2.5.5-203) and are considerably greater than the required minimum value of 1.1. These results demonstrate that the seismic performance of analyzed slopes is acceptable and that no seismically induced permanent slope displacement is expected at CPNPP Units 3 and 4 site. RCOL2_02.05.05-1

A liquefaction potential evaluation, as discussed in Subsection 2.5.4.8, indicates that the native rock material supporting all seismic category I and II structures and the engineered compacted fill surrounding the structures are not susceptible to soil liquefaction and there is no impact on any safety related structures.

The post-construction cut slopes around the west and south periphery of the CPNPP Units 3 and 4 site presented in Table 2.5.5-201 and shown on Figure 2.5.5-204, are not considered to pose any slope stability issues or hazards to seismic category I and II structures. The closest approach between the toe of the cut slopes and seismic category I or II structures is approximately 150 ft, with a minimum ratio of at least three times the height of slope, providing a substantial safety setback from the cut slopes. Additionally, the inclination of cut slopes is generally 2(H):1(V) or flatter. Considering the strength properties of the materials comprising the cut slopes (residual soil over Glen Rose Formation rock) and the maximum inclination of 2(H):1(V), all these cut slopes are considered to be inherently stable.

All safety-related plant structures are supported by foundations bearing into the competent Glen Rose Formation Layer C limestone below the plant grade at elevation of about 782 ft, and do not use any of the adjacent slopes or embankments for support. As a result, embankments or fill slopes around the perimeter of the plant do not affect the stability or performance of the safety-related structures.

2.5.5.3 Logs of Borings

The slope stability analyses incorporated relevant exploratory boring information, and derivative laboratory test data from these borehole samples, as described in

2.5-422 Hoek, E. and Diederichs, M.S. (2006), Empirical Estimation of Rock Mass Modulus, International Journal of Rock Mechanics & Mining Science 43, pages 203-215. (Copyrighted Material)

2.5-423 Obert, L. and Duvall, W.I. (1967), Rock Mechanics and the Design of Structures in Rock, John Wiley & Sons, Inc., NY. (Copyrighted Material)

2.5-424 Caterpillar (2006), Caterpillar Performance Handbook, Edition 36. (Copyrighted Material)

2.5-425 ~~Makdisi, F. and Seed, H.B. (1978), Simplified Method for Estimating Dam and Embankment-Induced Deformation, Journal of the Geotechnical Engineering Division, ASCE, July 1978, pages 849-867. (Copyrighted Material)~~ RCOL2_02.05.05-1

2.5-426 U.S. Army Corps of Engineers (2003), Slope Stability Manual, EM1110-2-1902, October 31, 2003.

2.5-427 ~~Bray, J.D., Travasarou, T. (2007), Simplified Procedure for Estimating Earthquake-Induced Deviatoric Slope Displacements, Journal of Geotechnical and Environmental Engineering, ASCE, 2007. (Copyrighted Material)~~ RCOL2_02.05.05-1

2.5-428 Janbu, N. (1968), Slope Stability Computations, Soils Mechanics and Foundation Engineering, the Technical University of Norway. (Copyrighted Material)

2.5-429 Janbu, N. (1973), Slope Stability Computations, Embankment Dam Engineering - Casagrande Volume, R.C. Hirschfield and S.J. Poulos, eds., John Wiley and Sons, New York, pp 47-86. (Copyrighted Material)

2.5-430 Bishop, A.W. (1955), The Use of the Slip Circle in the Stability Analysis of Slopes, Geotechnique, Vol 5, No. 1, pp 7-17. (Copyrighted Material)

2.5-431 Spencer, E. (1967), A Method of Analysis of the Stability of Embankments Assuming Inter-Slice Forces, Geotechnique, Vol 17, No. 1, pp 11-26. (Copyrighted Material)

2.5-432 Toro, C.R. (1996). Probabilistic Models of Site Velocity Profiles for Generic and Site-Specific Ground Motion Amplification Studies. Published as an appendix in Silva, W.J., N. Abrahamson, G. Toro and C. Costantino. (1997). "Description and validation of the stochastic ground motion model." Report Submitted to Brookhaven National Laboratory, Associated Universities, Inc. Upton, New York 11973, Contract No. 770573. CTS-00515

CP COL 2.5(1)

Table 2.5.5-203
Summary of Stability Analyses

RCOL2_02.05.05-1

Cases	Cross Section	Static Slope Stability Factor of Safety	~~Yield Acceleration, a_y (g)~~Pseudo-static Slope Stability Factor of Safety
Permanent	D-D'	2.80	~~0.44~~1.96
Permanent	E-E'	2.06	~~0.43~~1.66
Permanent	E1-E1'	1.93	~~0.37~~1.47
Permanent	F-F'	2.14	~~0.31~~1.56

RCOL2_02
.05.05-1

D-D'_seismic_(+)hor_(-)ver
Method: Spencer
Horizontal seismic coeff. Value: 0.1
Vertical seismic coeff. Value: -0.1
Compacted Fill Strength: C=200 psf, Phi=32 deg
Shale Strength: Fully-Softened Lower Bound (Shear-Normal Function)
Limestone Strength: Hoek-Brown Lower Bound (Shear-Normal Function)
Concrete Strength: C=5000 psf, Phi=0 deg
UHS Load: 3610 psf
Traffic Load: 250 psf

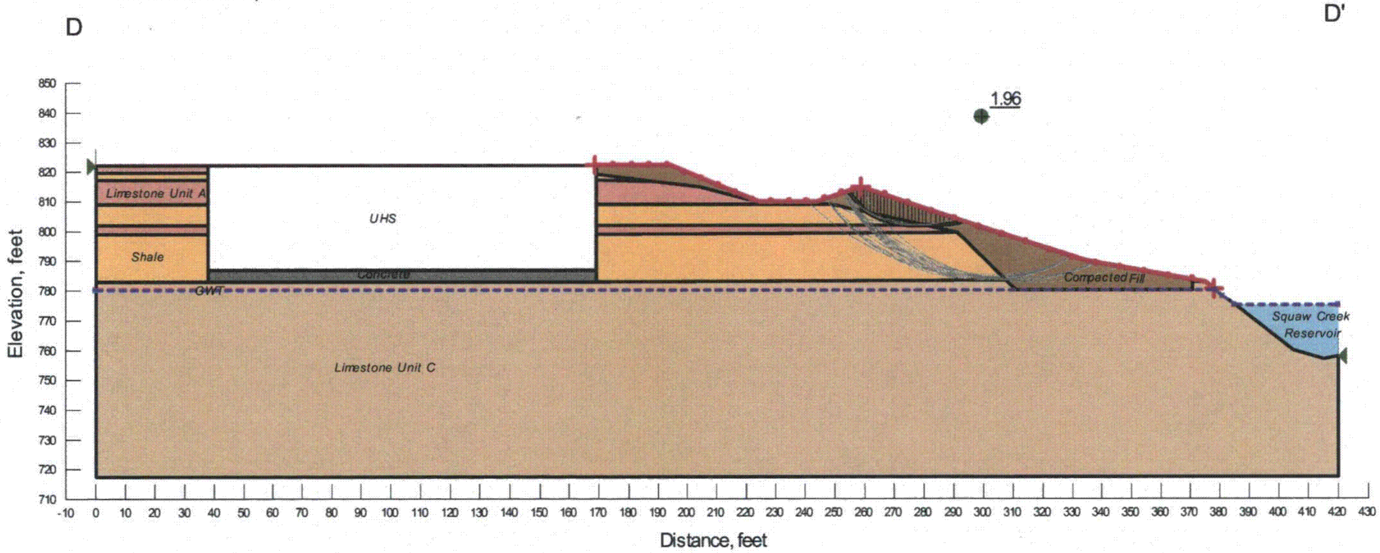

Figure 2.5.5-213 Seismic Stability Analysis- Cross Section D–D'

RCOL2_02.05.05-1

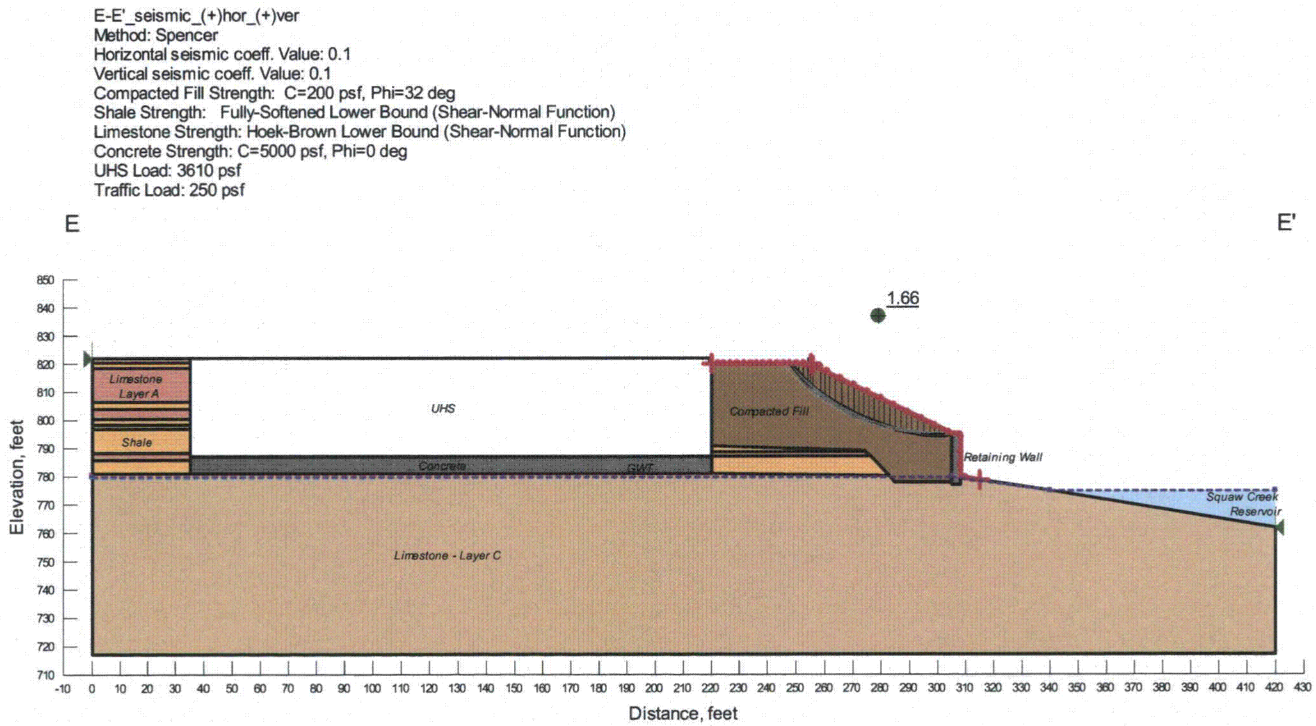

Figure 2.5.5-214 Seismic Stability Analysis- Cross Section E–E'

RCOL2_02.05.05-1

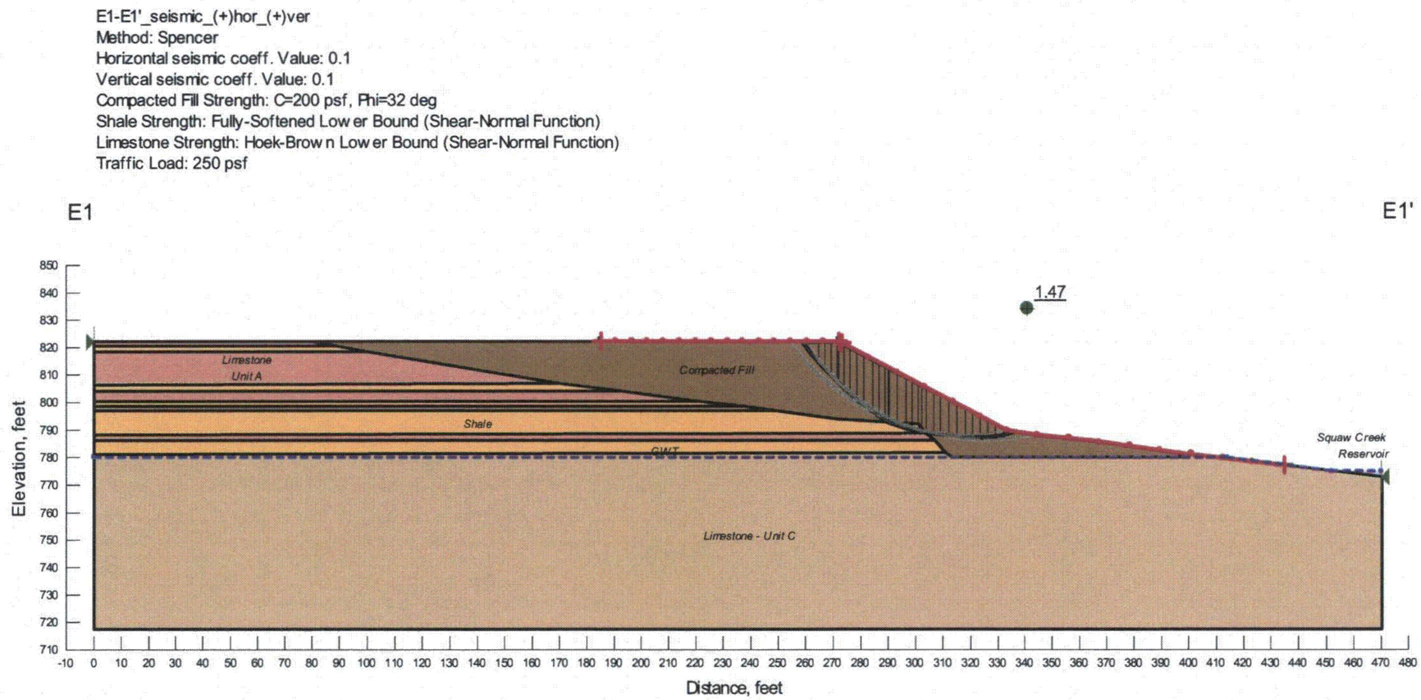

Figure 2.5.5-215 Seismic Stability Analysis- Cross Section E1–E1'

RCOL2_02
.05.05-1

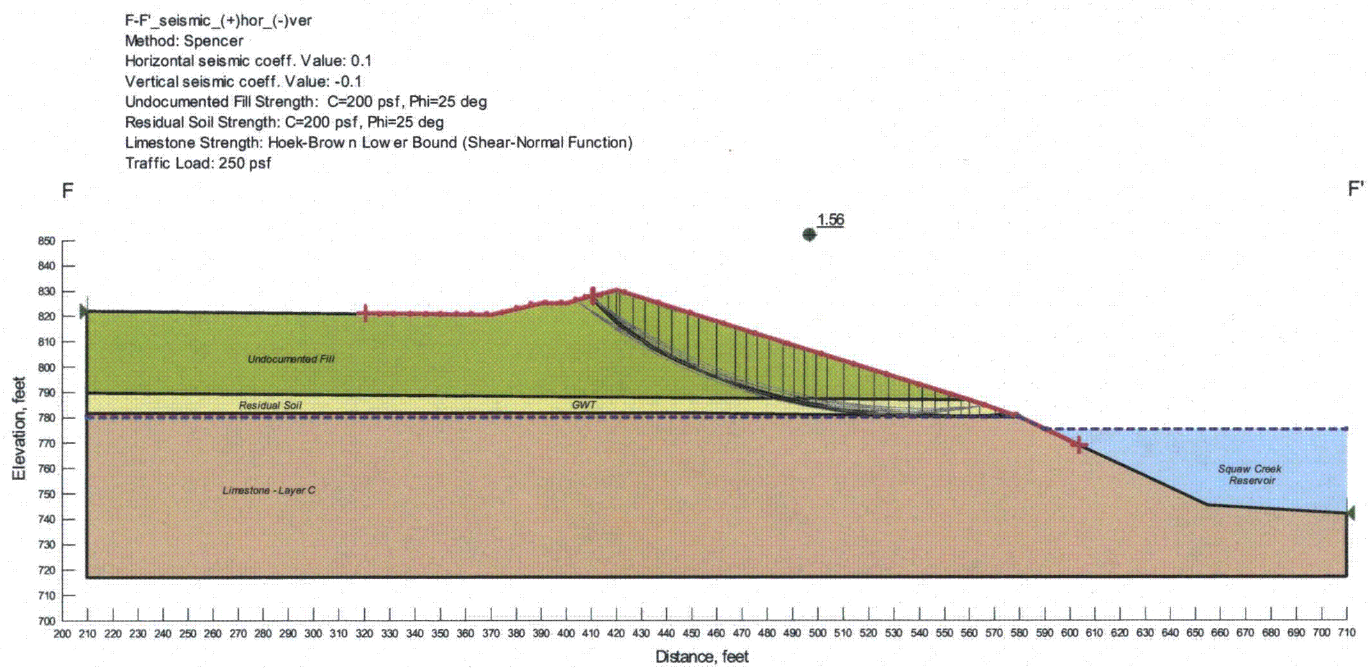

Figure 2.5.5-216 Seismic Stability Analysis- Cross Section F–F'

Attachment 4

TXUT-001-FSAR-2 5-CALC-009 Rev.1 - Settlement and Bearing Capacity (on CD)